SEMMELWEIS EGYETEM

DOKTORI ISKOLA

Ph.D. értekezések

3215.

GERGELY TAMÁS

Experimentális és klinikai farmakológia

című program

Programvezető: Dr. Szökő Éva, egyetemi tanár

Témavezetők: Dr. Varga Zoltán, egyetemi docens
Dr. Giricz Zoltán, tudományos főmunkatárs

INVESTIGATION OF DRUG-INDUCED CARDIOTOXICITY IN PRECLINICAL MODELS: FOCUSING ON CARDIO-ONCOLOGY AND HIDDEN CARDIOTOXICITY

PhD thesis

Tamás Gergely, MD

Semmelweis University Doctoral School

Pharmaceutical Sciences and Health Technologies Division

Supervisors: Zoltán Varga MD, PhD and Zoltán Giricz, PharmD, PhD

Official reviewers: Zoltán Pozsonyi, MD, PhD
Dániel Czuriga, MD, PhD

Head of the Complex Examination Committee: Éva Szökő, PharmD, DSc

Members of the Complex Examination Committee: Zoltán Jakus, MD, PhD
Ágnes Czikora, PhD

Budapest

2025

TABLE OF CONTENTS

LIST OF ABBREVIATIONS

AAR	area at risk
ACLY	ATP-citrate lyase
ACSVL1	very long-chain acyl-CoA synthetase
AMPK	AMP-activated protein kinase
ANOVA	analysis of variance
APC	antigen-presenting cell
ASCVD	atherosclerotic cardiovascular disease
BA	bempedoic acid
CAR-T cell	chimeric antigen receptor T cell
CLEAR	Cholesterol Lowering via BEmpedoic Acid, an ACL-inhibiting Regimen
CON	control
COX-2	cyclooxigenase-2
CSA	cross-sectional area
CTLA-4	cytotoxic T-lymphocyte-associated protein 4
CV	cardiovascular
CXCL9	chemokine (C-X-C motif) ligand 9
CXCR3	C–X–C motif chemokine receptor 3
ECG	electrocardiogram
EF	ejection fraction
FDA	Food and Drug Administration
GLS	global longitudinal strain
GO	gene ontology
HER2	human epidermal growth factor receptor 2
HF	heart failure
HFA-ICOS	Heart Failure Association - International Cardio-Oncology Society
HFpEF	heart failure with preserved ejection fraction
HFrEF	heart failure with reduced ejection fraction

HMG-CoA	β-Hydroxy β-methylglutaryl-coenzyme A
hsCRP	high sensitivity C-reactive protein
I/R	ischemia/reperfusion
ICH	International Conference for Harmonization
ICI	immune checkpoints inhitibor
IL	interleukin
ILB4	isolectin B4
IPC	ischemic preconditioning
irAE	immune-related adverse event
LAD	left anterior descending coronary artery
LAG-3	lymphocyte activation gene 3 protein
LDL	low-density lipoprotein
LVEDV	left ventricular end-diastolic volume
LVESV	left ventricular end-systolic volume
LVIDd	left ventricular internal diameter in diastole
LVIDs	left ventricular internal diameter in systole
LVSD	left ventricular systolic dysfunction
MACE	major adverse cardiac events
MAFLD	metabolic-associated fatty liver disease
MEK	mitogen-activated protein kinase kinase
MHC	major histocompatibility complex
Min	minutes
NK	natural killer
PBS	phosphate-buffered saline
PCSK9	proprotein convertase subtilisin/kexin type 9
PD1	programmed cell death protein 1
PDL1	programmed cell death ligand 1
PFA	paraformaldehyde

PPARγ	peroxisome proliferator-activated receptor-γ
qRT-PCR	quantitative real time polymerase chain reaction
RAF	rapidly accelerated fibrosarcoma
SCD	sudden cardiac death
SV	stroke volume
TCR	T cell receptor
VEGF	vascular endothelial growth factor
VTE	venous thromboembolism
WGA	wheat germ agglutinin

1 INTRODUCTION

1.1 Drug-induced cardiotoxicity in drug development and clinical practice

Drug-induced cardiotoxicity may present in many forms, including heart failure, increased risk of atherosclerotic cardiovascular disease (ASCVD), myocardial infarction, or arrhythmias leading to sudden cardiac death (1) (Figure 1). In this broad category, a distinction should be made between the cardiotoxic effects of oncological and non-oncological drugs: with oncological drugs, the cardiotoxic effects may be more common and related to their main mechanism of action, and may not be possible to uncouple from their anti-cancer effects. Due to this, cardiovascular risk stratification and potential cardioprotective strategies are needed in cancer patients, however, without interfering with the anti-cancer effects of the treatment. The significance of anti-cancer drug-induced cardiotoxicity is shown by the occurrence of a new interdisciplinary scientific field, cardio-oncology, which in part investigates the mechanisms of cardiotoxicity induced by anti-cancer drugs and potential strategies to alleviate these adverse effects. On the other hand, with non-oncological drugs, the cardiotoxic adverse effects are less common, however, they are one of the leading causes of post-marketing drug withdrawals (2,3). Screening studies for cardiotoxic effects are mandatory during drug development, nevertheless, drugs with cardiovascular adverse effects may still gain clinical approval due to undetected cardiotoxicity in preclinical and clinical studies – a phenomenon termed “hidden cardiotoxicity” (4). Hidden cardiotoxic effects of drugs may only manifest in the diseased hearts, e.g., during or after myocardial infarction, however, these conditions are currently not tested during drug development. Thus, improved preclinical testing systems are needed to identify hidden cardiotoxic effects at the early phases of drug development to decrease the number of patients at risk for these adverse effects in clinical trials and after marketization, in clinical practice.

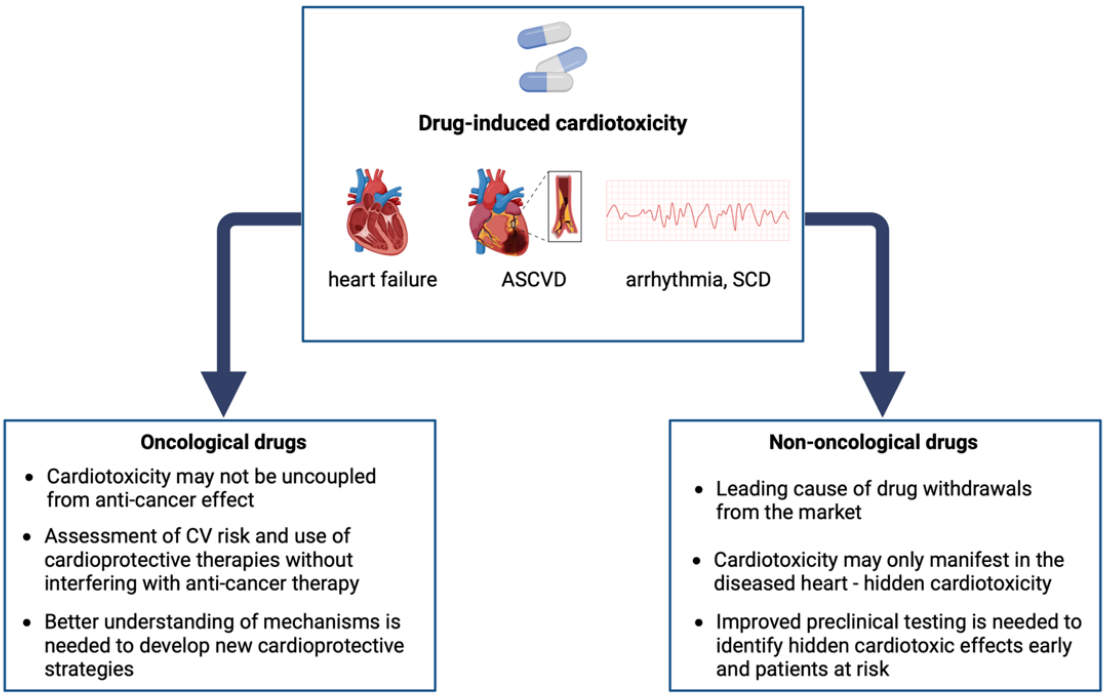

Figure 1. Manifestations of drug-induced cardiotoxicity and characteristic features of the cardiotoxicity of oncological and non-oncological medications. ASCVD, atherosclerotic cardiovascular disease; CV, cardiovascular; SCD, sudden cardiac death. *Created via. Biorender.com.*

1.2 Cardio-oncology: adverse effects of anti-cancer medications

1.2.1 Overview of the cardiotoxicity of different anti-cancer drug classes

Cardiotoxicity of anti-cancer medications is a long-known phenomenon (5,6), with a broad range of manifestations, including drug-induced heart failure and arrhythmias (7), as well as vascular toxicities (8). Importantly, cardiotoxicity of anti-cancer drugs is widespread, including classical chemotherapeutic agents (such as anthracyclines (9) and antimetabolites (10)) and newer, targeted therapies as well, such as anti-HER2 monoclonal antibodies (11) or small molecule signal transduction inhibitors (e.g., sunitinib, ibrutinib) (12). **More recently, cancer immunotherapy (such as immune checkpoint inhibitors and CAR-T cell therapy) has received widespread attention due to its breakthrough effect in the treatment of many cancer types, however, it has also become clear that even these novel therapies come with various cardiovascular adverse effects** (13,14). In the following chapters, we will discuss the biology and clinical relevance of immune checkpoint inhibitors, as well as the current knowledge on their cardiovascular toxicities.

1.2.2 Cardiotoxicity of immune checkpoint inhibitors

1.2.2.1 Immune checkpoint molecules

T cell activation requires at least two signals: (1) antigen presentation via T cell receptor (TCR) and major histocompatibility complex (MHC) and (2) co-stimulatory signaling, for example, by the interaction of CD28 and CD80/86 (15) (Figure 2). Immune checkpoint molecules are physiological regulators of immune activation (16).

Cytotoxic T-lymphocyte-associated protein 4 (CTLA-4) was the first immune checkpoint investigated thoroughly, a molecule with high similarity to CD28 (17). CTLA-4 is found in a variety of immune cells, including T cells, B-cells, natural killer (NK) cells, and dendritic cells (18). The most well-known function of CTLA-4 is its induced expression after T cell activation, to blunt the activation of the adaptive immune system (19). Its binding affinity to CD80 and CD86 is higher compared to CD28 (20,21), thus, when CTLA-4 is expressed on the cell surface, it can inhibit the co-stimulatory signal. Inhibition of CTLA-4 increases immune responses and represents a target for anti-cancer immunotherapy (17), while the use

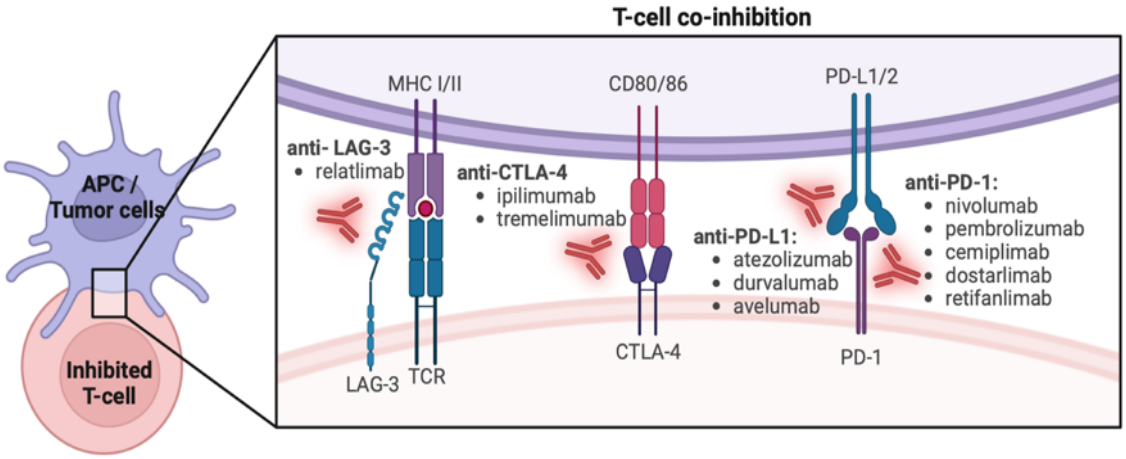

Figure 2. T cell co-inhibitory immune checkpoints and currently available immune checkpoint inhibitor monoclonal antibodies. APC, antigen-presenting cell; CTLA-4, cytotoxic T lymphocyte-associated protein 4; LAG-3, lymphocyte activation gene 3 protein; MHC, major histocompatibility complex; programmed cell death protein 1 (PD-1), programmed cell death ligand 1 (PD-L1), TCR, T cell receptor. *Adapted from Gergely et al., Nat. Rev. Cardiol., 2024* (53) . *Created via Biorender.com*

of CTLA-4-immunoglobulin fusion proteins (such as abatacept and belatacept) is useful for autoimmune diseases (22) and preventing solid organ transplant rejection (23).

Programmed cell death protein-1 (PD-1) and its ligand, PD-L1, were later discovered as further immune checkpoints, with effects distinct from CTLA-4 signaling (24). PD-1 is mainly expressed in immune cells, including T cells and myeloid cells, and is involved in peripheral tolerance development (25). PD-L1 is expressed on antigen-presenting cells (APCs), and it can also be found on non-hematological cell types, including endothelial cells and possibly cardiomyocytes (26). While immune checkpoints physiologically regulate immune cell activation to prevent autoimmune responses, upregulation of co-inhibitory checkpoints, such as PD-L1, is a common mechanism in tumour cells to escape immune surveillance and promote tumour survival (27), thus presenting a target for cancer immunotherapy.

1.2.2.2 Role of immune checkpoint inhibitors in oncology

Inhibition of the co-inhibitory immune checkpoint CTLA-4 with ipilimumab was demonstrated to result in tumour regression in a subset of patients with metastatic melanoma (28,29), and it was the first immune checkpoint inhibitor to gain Food and Drug Administration (FDA) approval in 2011. Since then, several ICIs targeting the PD-1 axis have been approved, such as nivolumab (30) or pembrolizumab (31), alone or in combination with CTLA-4 blockade (32,33). The indications for ICI treatment are quickly expanding, including metastatic melanoma, non-small cell lung cancer, renal cell carcinoma, Hodgkin's lymphoma, colorectal and bladder cancers, among many other cancer types. The use and importance of ICI therapy in cancer is rising rapidly: for instance, in 2021, 5863 ongoing clinical trials were investigating PD-1/PD-L1-targeted immunotherapies either alone or in combination treatments (34).

1.2.2.3 Cardiovascular adverse effects of immune checkpoint inhibitor therapy

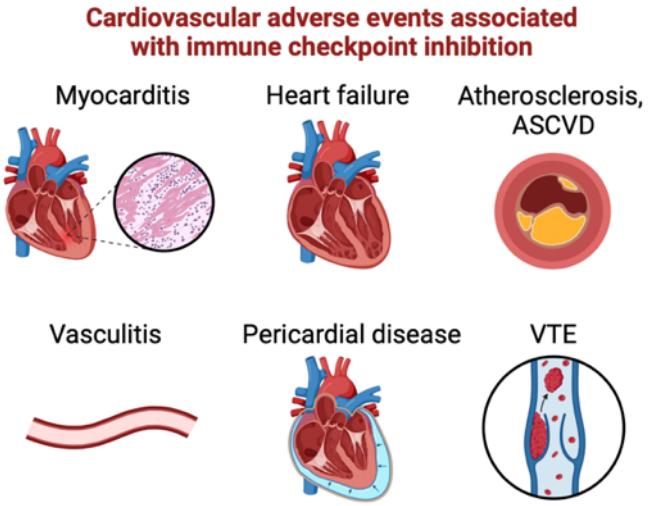

Figure 3. Cardiovascular toxicities associated with immune checkpoint inhibitors. ASCVD, atherosclerotic cardiovascular disease; VTE, venous thromboembolism. *Adapted from Gergely et al., Basic Res. Cardiol., 2024* (35). *Created via Biorender.com*

ICI therapy has been shown to induce several immune-related adverse events (irAE), that affect most tissues (36), including colitis (37), cutaneous toxicity (38), hepatotoxicity (39), endocrinopathies (such as hypophysitis (40) and thyroiditis (40)), neuropathy (41) and

nephritis (42). **Furthermore, several cardiovascular adverse effects have been observed after ICI therapy** (43–46) (Figure 3).

Overall, ICIs increase the occurrence of major adverse cardiac events (MACE) compared to non-ICI-based anti-cancer therapy in metastatic melanoma and lung cancer (47). Of these, ICI-induced myocarditis has been studied in the most detail, as it represents the most severe form of ICI-induced cardiac events, with up to 50% lethality (48). Nevertheless, ICI treatment has also been shown to accelerate atherosclerosis (49), lead to arrhythmias (50) and cardiac dysfunction, ranging from a milder, subclinical effect (51) to late-onset heart failure (52). Notably, heart failure without concomitant myocarditis is an emerging adverse effect of ICI therapy (53). Potential mechanisms leading to late cardiac dysfunction or heart failure include the persistence of cardiac inflammation ("smoldering myocarditis"), progression from acute to chronic heart failure, and the acceleration of atherosclerotic plaque development or rupture, leading to heart failure with ischemic etiology (53) (Figure 4).

Mechanisms of ICI-induced cardiotoxicity are not fully understood currently. Myocardial infiltration of immune cells (including $CD8^+$ and $CD4^+$ T cells, $CD68^+$ macrophages) has been shown in histological samples of ICI myocarditis (54–56), whereas clonal expansion of $CD8^+$ T cell populations specifically recognizing cardiac antigens, such as alpha-myosin, has been suggested as a potential mechanism for fulminant myocarditis development (57). Interestingly, MYH6, the gene encoding alpha-myosin, is not expressed in thymic epithelial cells, thus, autoreactive T cells may be present in the circulation in low numbers in healthy states (57). In naïve mice, these autoreactive T cells have been found in the myocardium with high expression of PD-1 (58), potentially suppressing autoimmune effects in homeostatic states. During immune checkpoint inhibition treatment, these T cell populations may become activated and target cardiac tissues. Nevertheless, myocarditis only occurs in 1% of patients, thus understanding of further risk factors is needed. Moreover, the central role of the thymus has been shown in myocarditis development after ICI treatment in a clinical study (59). **The mechanisms of other ICI-cardiotoxicities, including ICI-induced non-myocarditis heart failure, are far less understood** (35)**, highlighting the need for mechanistic investigation of these effects to understand the patients at risk and develop potential cardioprotective strategies.** Current treatment options for ICI cardiotoxicity include glucocorticoids for ICI

myocarditis, while in refractory cases, second-line immunosuppressive therapy is recommended, such as mycophenolate mofetil, anti-thymocyte globulin, tocilizumab, abatacept, alemtuzumab, and tofacitinib (60). Notably, abatacept, a CTLA-4 fusion protein, has been a promising therapeutic option in preclinical studies (61) and clinical reports (62,63), with ongoing clinical trials investigating its efficacy in ICI myocarditis (64). For early ICI-induced cardiac dysfunction, anti-TNFα therapy has been shown to improve cardiac function in a preclinical model (51), however, its clinical applicability may be limited as TNFα inhibitors are contraindicated in heart failure. **Nevertheless, there is a need for novel therapeutic options to alleviate the various forms of ICI cardiotoxicity.**

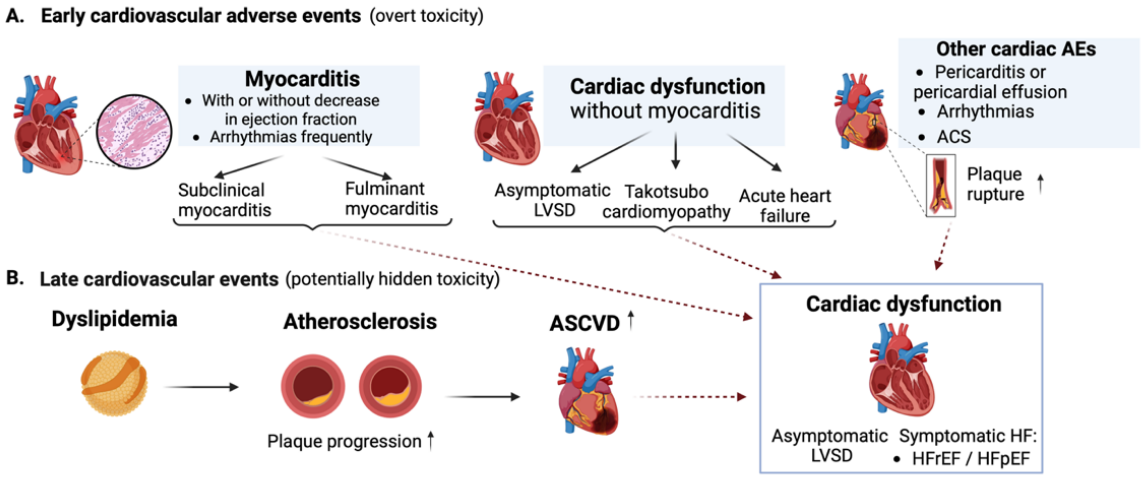

Figure 5. Early (A) and late (B) cardiovascular adverse events following ICI therapy. Dashed lines show potential pathways for late-onset cardiac dysfunction development. AE, adverse event; ASCVD, atherosclerotic cardiovascular disease; HF, heart failure; HFrEF, heart failure with reduced ejection fraction; HFpEF, heart failure with preserved ejection fraction, LVSD, left ventricular systolic dysfunction. *Adapted from Gergely et al., Nat. Rev. Cardiol., 2024 (53). Created via Biorender.com*

1.3 Cardiotoxicity of non-oncological drugs: the importance of hidden cardiotoxicity

Unexpected cardiac adverse events are one of the leading causes of drug withdrawals from the market (3). Drug-induced cardiovascular adverse effects can manifest in multiple forms, including arrhythmias and sudden cardiac death (65), myocardial infarction (66,67), heart failure (68), and valvular problems (69). In consequence of the high number of drug withdrawals due to cardiotoxicity, especially in the 1990s, significant efforts were made to improve cardiac safety testing during drug development in the early 2000s, resulting in recommendations by the International Conference for Harmonization (ICH) for the assessment of cardiac safety. In ICH S7A, testing of the pharmacodynamic properties of new investigational compounds is described, with cardiovascular effects investigated by blood pressure and heart rate measurements, electrocardiograms, as well as measurement of cardiac output or ventricular contractility (70). ICH S7B describes the non-clinical evaluations of the potential for delayed ventricular repolarization, including both *in vitro* and *in vivo* testing (71). **Nevertheless, even with these mandatory testing protocols, drug-induced cardiotoxicity may not always be detectable during drug development.**

1.3.1 Definition of hidden cardiotoxicity

The current preclinical cardiac safety testing protocols are mainly performed on young, healthy animals, or *in vitro* models without simulating pathological conditions. **However, some cardiovascular adverse effects may only manifest in the diseased heart or cardiomyocytes, a phenomenon termed "hidden cardiotoxicity"** (4)**.** These conditions can include, e.g., cardiac ischemia/reperfusion injury, or the presence of comorbidities, such as hypercholesterolemia or diabetes mellitus, which can alter the cellular processes in the heart. Mechanisms of hidden cardiotoxicity may include enhancement of cell death or proarrhythmic pathways during cardiac pathologies, e.g., ischemia/reperfusion injury, or interference with endogenous cardioprotective pathways (Figure 5, (4)). **Testing of new investigational compounds in the non-clinical phase may reveal hidden cardiotoxic effects early, thus enabling the identification of at-risk patients before clinical use** (4)**.**

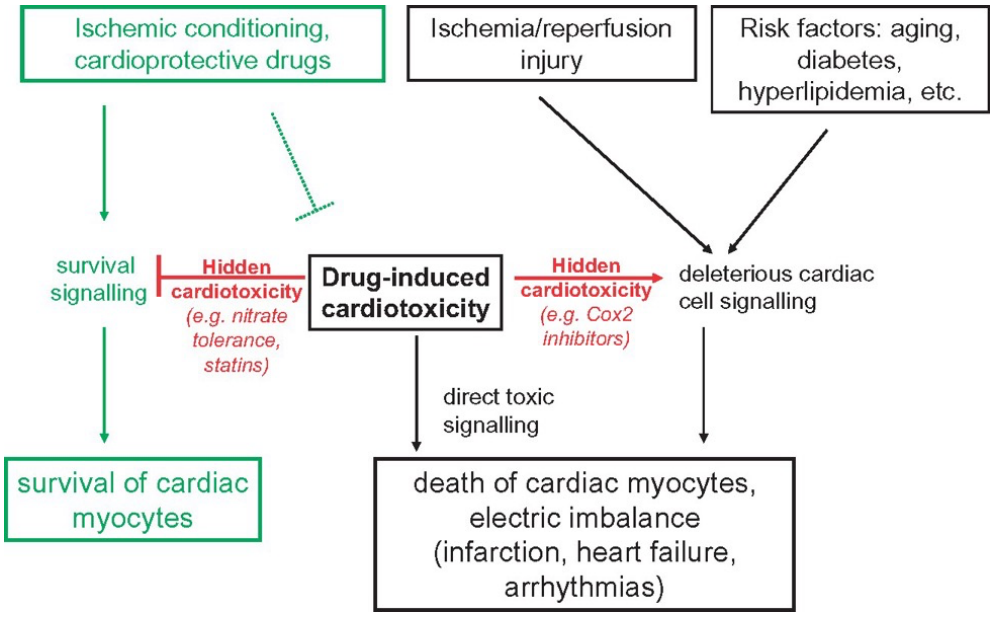

Figure 6. Mechanisms of hidden cardiotoxicity. Hidden drug-induced cardiotoxicity may be caused by interference with the endogenous survival signaling of the cardiac myocytes or by enhancing the deleterious cardiac signaling in the diseased heart, e.g., during ischemia/reperfusion injury or in the presence of cardiometabolic risk factors. *Adapted from Ferdinandy et al., Eur. Heart J., 2019* (4)

1.3.2 Drug-induced hidden cardiotoxicity in the clinical setting

The need for testing of novel compounds for hidden cardiotoxic effects is highlighted by the fact that current preclinical testing systems do not investigate novel compounds in diseased hearts, whereas in phase II / III clinical trials safety results may not be generalizable to all patients with cardiac diseases and comorbidities due to strict exclusion and inclusion criteria of the studies. Cardiovascular toxicities may only become evident during post-marketing phase IV trials involving assessment of cardiovascular outcomes, as was the case with the selective cyclooxygenase-2 (COX-2) inhibitor rofecoxib, where the increased cardiovascular risk was observed in post-marketing clinical studies (72,73), ultimately leading to its withdrawal from the market 5 years after authorization. Similarly, the PPARγ agonist antidiabetic drug rosiglitazone was found to increase the risk of myocardial infarction in a meta-analysis (67) after its market authorization. Rosiglitazone improves HbA1c levels, a

surrogate for blood glucose control, however, its effects on cardiovascular outcomes were not fully known at the time of approval. The findings of the meta-analysis (67) led to regulatory actions, restricting its clinical use (74). Since the findings that rosiglitazone increased cardiovascular risk despite optimal glucose control, new guidelines were set in place, requiring that all investigational antidiabetic drugs undergo a cardiovascular outcome trial before market authorization (75).

Nevertheless, other drug classes aimed for the treatment of cardiovascular co-morbidities, such as antihyperlipidemic drugs, can still be authorized based on the reduction of surrogate markers (e.g. LDL-cholesterol) and do not require outcome trials prior to marketization, thus potentially some cardiovascular adverse effects may remain hidden and could only be revealed in post-marketing phase IV studies.

1.3.3 Preclinical testing of drug-induced hidden cardiotoxicity

Our research group has investigated hidden cardiotoxicity in multiple preclinical models previously. First, we tested the cardiotoxic properties of rofecoxib, a selective COX-2 inhibitor, which was withdrawn from the market due to its cardiovascular effects. In a rat model of acute myocardial ischemia/reperfusion injury, rofecoxib was found to increase the occurrence of lethal ventricular arrhythmias during ischemia/reperfusion, which effect was not seen in healthy hearts, showing its hidden cardiotoxic properties (76). In another study, we tested rosiglitazone, a thiazolidinedione class antidiabetic withdrawn from the market due to an increased risk of myocardial infarction (67). In this study, we found no evidence of hidden cardiotoxicity, but rosiglitazone interacted with the cardioprotective effects of ischemic preconditioning, abolishing its arrhythmia-reducing effect (77).

1.3.4 Bempedoic acid, a novel lipid-lowering drug with unknown effects during cardiac ischemia

Bempedoic acid is a novel, first-in-class antihyperlipidemic drug. Its main targets include ATP-citrate lyase (ACLY), an enzyme upstream of HMG-CoA reductase (the target of statins) in the endogenous cholesterol synthesis pathway (78) (Figure 6). Inhibition of ACLY leads to decreased cholesterol production by the hepatocytes, with subsequent expression of LDL-receptors on the surface, ultimately leading to decreased LDL-cholesterol levels in the

circulation (79). Preclinical studies have shown that bempedoic acid is a prodrug, activated and effective only in the liver for ACLY inhibition, but not in the skeletal muscle (79), thus potentially leading to fewer muscle-related adverse effects, the most common reason for statin intolerance (80,81). Other mechanisms of bempedoic acid include enhancing AMPK signaling (82) and reducing inflammation (83).

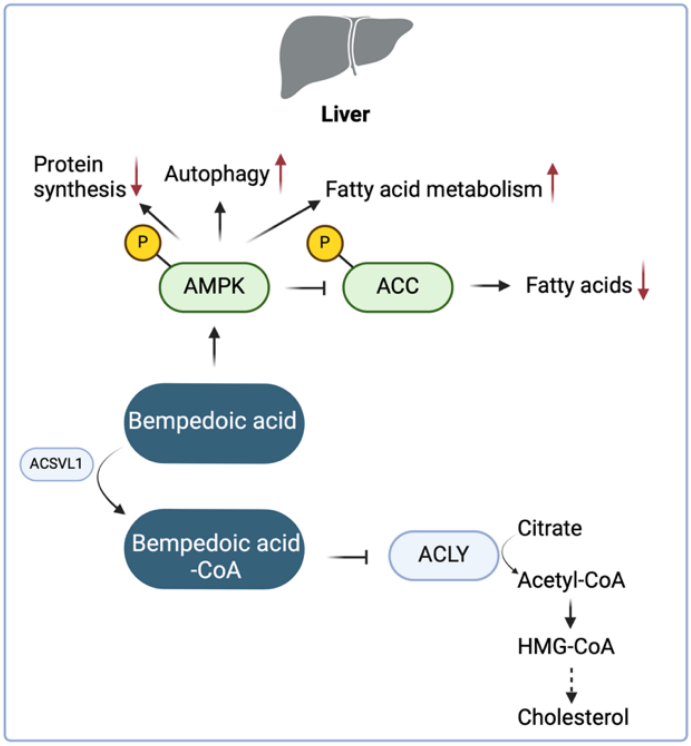

Figure 7. Mechanism of action of bempedoic acid in the liver. Bempedoic acid is activated by the very long-chain acyl-CoA synthetase (ACSVL1) enzyme, expressed in hepatocytes but not in skeletal muscle cells. Activated bempedoic acid (bempedoic acid-coenzyme A) is needed for the inhibition of ATP citrate lyase (ACLY) and downstream effects resulting in decreased endogenous cholesterol synthesis. Based on preclinical studies, bempedoic acid may lead to the phosphorylation of AMP-activated protein kinase (AMPK) in its free acid form as well, with subsequent downstream effects, including inhibition of acetyl-CoA carboxylase, altogether increasing autophagy and fatty acid metabolism while decreasing protein synthesis and fatty acid levels. *Created via Biorender.com*

Bempedoic acid received marketing authorization in 2020 by the Food and Drug Administration and the European Medicines Agency, after clinical studies showing its ability to reduce LDL-cholesterol in the CLEAR (Cholesterol Lowering via BEmpedoic Acid, an ACL-inhibiting Regimen) studies (84), nevertheless, its effects on cardiovascular outcomes were not known at the time of marketization. Since then, the CLEAR Outcomes trial showed a decrease in major adverse cardiac events with bempedoic acid use in statin-intolerant patients (85). Interestingly, in subsequent analysis, bempedoic acid was shown to be more efficient in primary prevention (in patients without established cardiovascular disease) (86). Furthermore, in a post-hoc analysis using Bayesian methods, the beneficial effects of bempedoic acid in secondary prevention (in patients with already established cardiovascular disease) were more modest, and a potential increase in all-cause and cardiovascular mortality was also observed (87). **These findings suggest that the cardiovascular effects of bempedoic acid may be altered in patients with diseased hearts. Bempedoic acid has not been investigated previously in preclinical models of ischemic heart disease, e.g., ischemia/reperfusion injury, thus, mechanistic investigation for hidden cardiotoxic effects is warranted (Figure 7).**

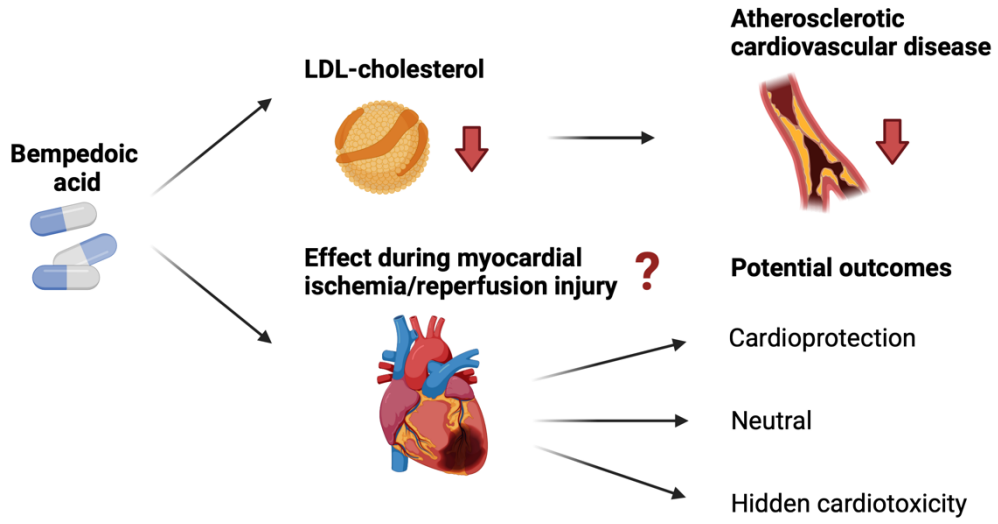

Figure 7. Known and potential cardiovascular effects of bempedoic acid. Although bempedoic acid was shown to reduce low-density lipoprotein (LDL)-cholesterol and decrease atherosclerotic cardiovascular disease, its effects during acute myocardial ischemia/reperfusion injury have not been investigated before. *Created via Biorender.com*

2 OBJECTIVES

The field of drug-induced cardiotoxicity poses many unanswered questions, ranging from basic science to clinical practice. The cardiotoxicity of novel anti-cancer medications is incompletely understood, whereas deeper insights into the molecular mechanisms are needed to develop successful cardioprotective therapies. Moreover, evaluating the hidden cardiotoxic properties of non-oncological drugs is pivotal for preventing unexpected cardiotoxic events, especially in the case of medications indicated for the treatment of cardiovascular risk factors, as these patients may already be at a higher risk for developing cardiovascular disease.

Here, we aimed to investigate two emerging topics in the field of drug-induced cardiotoxicity:

(1) In our first study, we aimed to investigate the mechanisms of anti-PD-1 immune checkpoint inhibitor-induced cardiotoxicity in a mouse model, to find molecular targets for ameliorating adverse cardiovascular events.

(2) In our second study, we aimed to investigate the potential hidden cardiotoxic properties of the novel antihyperlipidemic drug, bempedoic acid, in a rat model of acute myocardial ischemia/reperfusion injury.

3 METHODS

For the full methodical descriptions, please see the corresponding publications (88,89).

3.1 Ethical approvals and animal welfare

All procedures were approved by the National Scientific Ethical Committee on Animal Experimentation and the Semmelweis University's Institutional Animal Care and Use Committee (H-1089 Budapest, Hungary) in accordance with NIH guidelines (National Research Council [2011], Guide for the Care and Use of Laboratory Animals: Eighth Edition) and permitted by the government of Food Chain Safety and Animal Health Directorate of the Government Office for Pest County (project identification code: PE/EA/1912-7/2017; date of approval: November 2017). The animals had an acclimatization period of at least 1 week prior to experiments. Mice and rats were maintained under a 12:12 h light–dark cycle, under controlled environmental conditions (20–24 °C and 35–75% relative humidity) in individually ventilated cages with shelters, holding two to four animals per cage. Standard rodent chow and tap water were provided ad libitum throughout the entire study. Animal studies were reported in compliance with the ARRIVE guidelines (90).

3.2 Preclinical model of immune checkpoint inhibitor-induced cardiotoxicity

3.2.1 In vivo experiments

C57BL/6J and BALB/c mice (ranging from 8 to 10 weeks in age and weighing 20–28 g at the beginning of the study) were randomly assigned to isotype control or anti-PD-1 treated groups, using a strategy to minimize initial weight difference between study groups. The following antibodies were used for in vivo treatments (all purchased from BioXCell, Lebanon, NH, USA): anti-PD-1 monoclonal antibody (clone RMP1-14, BP0146), anti-CD4 (clone GK1.5, BP0003), anti-IL17A (clone 17F3, BP0173), and isotype control (rat IgG2a, clone 2A3, BP0089). C57BL/6J mice were treated three times a week for either 2 or 4 weeks with a dose of 200 μg per mouse (n = 10 per group, Figure 8/A), whereas BALB/c mice were treated for three times a week for 2 weeks with a dose of 200 μg per mouse (n = 10 per group, Figure 8/B). In separate experiments, C57BL6/J mice were randomly assigned to isotype

control, anti-PD-1, anti-CD4, or anti-IL17A-treated groups (200 µg per mouse, n = 10 per group, Figure 8/C). The initial group size calculation was performed based on left ventricular ejection fraction (EF) as the primary endpoint. Assuming 65% as the control group's EF (based on previous measurements with a typical standard deviation ±5), at least eight animals per group were needed to detect at least a 10% decrease with a power of 0.8 and alpha = 0.05. We chose an initial number of 10 animals per group to account for unexpected mortality and technical issues. After the treatment period, cardiac function was evaluated by echocardiography. Following this, mice were sacrificed under ketamine/xylazine anesthesia (100/10 mg/kg) with cervical dislocation, followed by whole-body perfusion with phosphate-buffered saline (PBS), after which organs were stored for histological and molecular analyses.

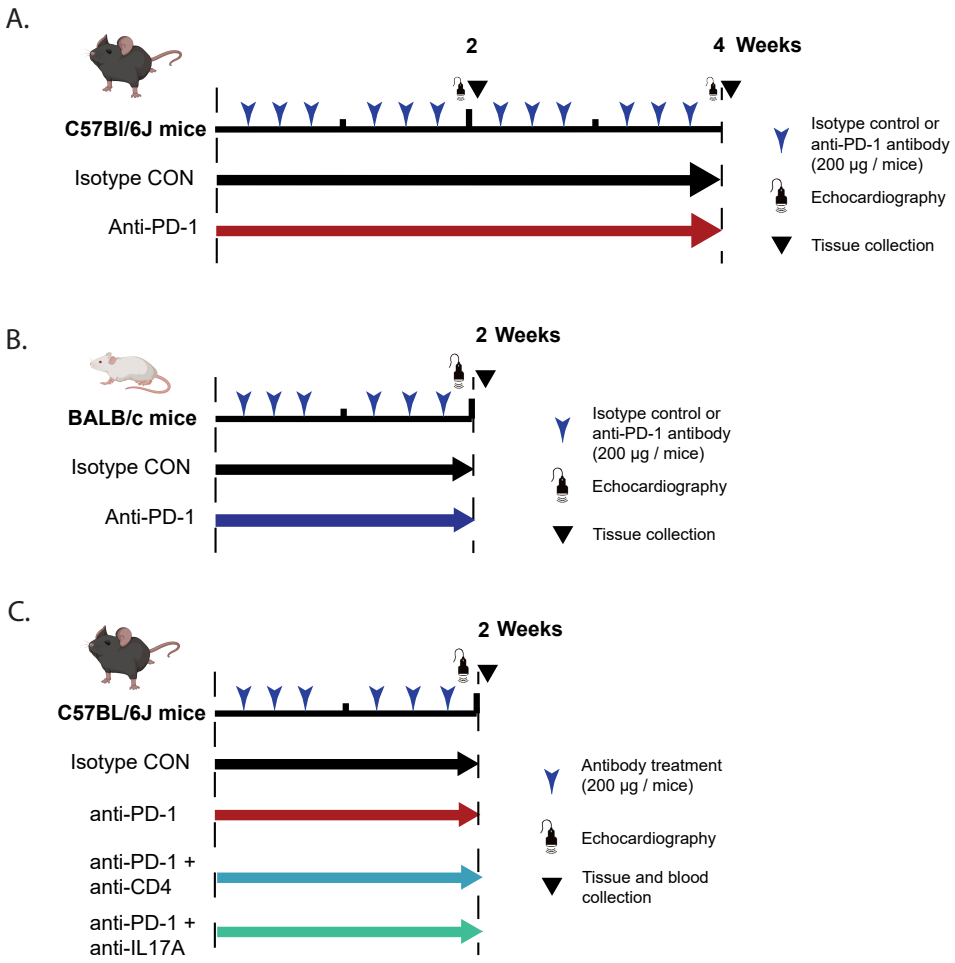

Figure 8. Schematic protocols for the in vivo experiments. (A) Treatment of C57BL/6J mice with anti-PD-1 or isotype control antibodies for either 2 or 4 weeks. (B) Treatment of BALB/c mice with anti-PD-1 or isotype control antibodies for 2 weeks. (C) Treatment of C57BL/6J mice with isotype control, anti-PD-1, anti-PD-1 + anti-CD4 or anti-PD-1 + anti-IL17A antibodies for 2 weeks. *Adapted from Gergely et al., Br. J. Pharm., 2023* (89)

3.2.2 Echocardiography

Mice were anaesthetized with isoflurane (5% for induction, 2% for maintenance) and placed on heating pads to maintain 37 °C body temperature, with continuous monitoring of core temperature via a rectally placed probe. Echocardiographic analysis was done with the Vevo 3100 high-resolution in vivo imaging system (Fujifilm VisualSonics, Toronto, Canada) using an ultrahigh-frequency MX400 transducer (30 MHz, 55 frames per second) by an operator blinded to the study groups. On two-dimensional recordings of the short-axis at the mid-papillary muscle level, measured parameters included left ventricular internal diameter in systole and diastole (LVIDs and LVIDd, respectively), LV anterior wall thickness, and posterior wall thickness. End-diastolic and end-systolic LV areas were measured from short- and long-axis two-dimensional B-mode recordings. Diastolic parameters were measured in the apical four-chamber view. Pulsed-wave Doppler and tissue Doppler were used to determine early mitral inflow velocity (E) and mitral annular early diastolic velocity (e'), respectively. Fractional shortening was calculated as [(LVIDd - LVIDs)/ LVIDd] × 100. End-diastolic (LVEDV) and end-systolic (LVESV) LV volumes were calculated from the rotational volumes of the left ventricular trace at the diastole and systole around the long axis line of the spline. Stroke volume (SV) was calculated as LVEDV × LVESV. Ejection fraction (EF) was determined as (SV/LVEDV) x 100. Cardiac output was calculated as (SV × HR/1000). LV mass was calculated according to a cubic formula, proposed first by Devereux et al. (1986) and modified for rodents (91) (LV mass = 1.04 × [(LVIDd + LVAWd + LVPWd)^3 × LVIDd^3] × 0.8 + 0.6). An evaluator blinded to the study groups evaluated echocardiographic recordings via VevoLAB software (Fujifilm VisualSonics, Toronto, Canada). Global longitudinal strain (GLS) was assessed by speckle-tracking. Two to three consecutive cardiac cycles in B-mode were selected for this procedure. Using the Vevo Strain

Software, semi-automated tracing of the endocardial and epicardial borders in the parasternal long-axis was performed to calculate GLS. Papillary muscles were excluded from the GLS analysis. Mice with a high respiratory rate, which prevented tracing consecutive cardiac cycles, were excluded from GLS analysis.

3.2.3 Histology

Heart tissues were fixed in neutral buffered formalin for 24 h, then dehydrated in alcohols, and embedded in paraffin. 5 μm-thick sections were used for histological analyses and immunohistochemistry.

Hematoxylin and eosin staining. Paraffin-embedded heart sections were stained with hematoxylin and counterstained with eosin, after initial de-paraffinization and hydration for evaluation of morphologic and pathologic alterations.

Sirius red staining. Heart sections after initial preparations (see above) were pre-treated with 0.2% aqueous phosphomolybdic acid, followed by staining with 0.0125% picrosirius red for 1 h, and then washed with 0.01 N HCl. The extent of cardiac fibrosis was analyzed and quantified by ImageJ Software, using predefined threshold values, in a blinded manner.

Immunohistochemistry. Prepared heart sections underwent antigen retrieval in a citrate-based solution for 30 min. After blocking endogenous peroxidase activity via 3% H2O2 in PBS solution, the sections were blocked with 2.5% goat serum in PBS and 2.5% milk powder. Primary anti-CD3ε antibodies (rabbit IgG, 85061, Cell Signaling Technology, Technology, Leiden, The Netherlands) were diluted (1:200) in goat serum (2.5%) and were incubated overnight at 4 °C. After washing with gentle shaking three times with PBS, the sections were incubated with anti-rabbit IgG secondary antibodies (8114S, Cell Signaling Technology, Leiden, The Netherlands) conjugated with horseradish peroxidase. Secondary antibodies were washed with gentle shaking three times with PBS, and signals were developed with diaminobenzidine (SK-4103, ImmPACT DAB EqV Peroxidase [HRP] Substrate, Vector Laboratories, Burlingame, CA, USA). CD3ε-positive cells were counted manually by an evaluator blinded to study groups.

Lectin histochemistry. Prepared heart sections underwent antigen retrieval in an alkaline solution for 30 min. The sections were incubated with wheat germ agglutinin (WGA-FITC,

1:50, Sigma Aldrich, L4895) and isolectin B4 (ILB4-DyLight 594, 1:50, Invitrogen, L32473) overnight at 4 °C (92). Cardiomyocyte cross-sectional area was analyzed by automatically delineating cross sections of cardiomyocytes with ImageJ Software, by an evaluator blinded to study groups. Cardiomyocytes were analyzed on at least eight images per heart. Microvascular density was calculated as the ratio of microvascular count divided by the average cross-sectional area of the cardiomyocytes.

3.2.4 RNA isolation and quantitative reverse transcription-polymerase chain reaction (qRT-PCR)

Total RNA was isolated from mouse heart, thymus, and spleen samples with a chloroform/isopropanol precipitation method. Qiazol® (Qiagen, The Netherlands) was added to each sample and homogenized with TissueLyser (Qiagen, The Netherlands). Homogenates were centrifuged, and from the clean upper phase, DNA and protein were precipitated with chloroform. Total RNA was precipitated with isopropanol, and pellets were washed four times with 75% ethanol (vWR, PA, USA). Finally, total RNA was resuspended in nuclease-free water, and the RNA concentration was determined by spectrophotometry (Implen Nanophotometer® N60, München, Germany). cDNA was synthesized from 1 µg total RNA by Sensifast cDNA synthesis kit (Bioline, UK) according to the manufacturer's protocol. cDNA was further diluted 20x with RNAse-free water. qRT-PCR reactions were performed on a LightCycler® 480 II instrument (Roche, Germany) by using SensiFAST SYBR Green master mix (Bioline, UK). Peptidylprolyl isomerase A (Ppia) and ribosomal protein L13a (Rpl13a) were used as housekeeping genes. Results were calculated with $2^{-\Delta\Delta Cp}$ evaluation method.

3.2.5 RNA sequencing and bioinformatics analysis

RNA sequencing. The RNA Integrity Numbers and RNA concentration were determined by RNA ScreenTape system with 2200 Tapestation (Agilent Technologies, Santa Clara, CA, USA) and RNA HS Assay Kit with Qubit 3.0 Fluorometer (Thermo Fisher Scientific, Waltham, MA, USA), respectively. For gene expression profiling (GEx) library construction, Quant-Seq 3' mRNA-Seq Library Prep Kit FWD for Illumina (Lexogen GmbH, Wien, Austria) was applied according to the manufacturer's protocol. The quality and quantity of

the library were determined by using High Sensitivity DNA1000 ScreenTape system with the 2200 Tapestation (Agilent Technologies, Santa Clara, CA, USA) and dsDNA HS Assay Kit with the Qubit 3.0 Fluorometer (Thermo Fisher Scientific, Waltham, MA, USA), respectively. Pooled libraries were diluted to 2 pM for 1x86 bp single-end sequencing with 75-cycle High Output v2.5 Kit on the NextSeq 500 Sequencing System (Illumina, San Diego, CA, USA) according to the manufacturer's protocol. Datasets from the RNA sequencing experiments are publicly available at ArrayExpress (https://www.ebi.ac.uk/biostudies/arrayexpress) under the accession number E-MTAB-12388.

Bioinformatics analysis. To perform adapter and poly(A) tail trimming, quality- and length-filtering of raw RNA sequencing reads, we used Cutadapt software (version 2.10) (93). Reads with a Phred quality score below 30, or reads with a length of less than 19 nucleotides were filtered out. For quality control analysis, we used FastQC (version 0.11.9) and MultiQC (version 1.10) (94) tools. Adapter-trimmed and filtered reads were aligned to the GRCm38 Mus musculus reference genome assembly (Ensemble release 81) (95) using HISAT2 software (version 2.2.1) (96). Annotation and read counting were performed by featureCounts (version 2.0.1) (97) using the corresponding reference annotation. Normalization, differential expression analysis of the annotated reads, and visualizations of the results by volcano plots were conducted with the use of the DESeq2 (version 1.10.1) (98) Bioconductor package and custom scripts developed in the R programming language (version 3.2.3). To control false discovery rate due to multiple hypothesis testing, p values of pairwise comparisons were corrected by the Benjamini–Hochberg procedure, yielding q values (99).

Gene Ontology enrichment analysis. We performed Gene Ontology (database version released on 9 October 2020) enrichment analysis against the Mus musculus reference gene list, using the online PANTHER Overrepresentation Test (geneontology.org, version released on 28 July 2020) (100) to evaluate enriched biological process terms among genes that were significantly differentially expressed based on non-corrected p values. Enrichment p values were assessed with Fisher's exact test, and results were corrected for multiple comparisons by applying the false discovery rate method.

3.2.6 Flow cytometry

After sacrifice, the thymus and spleen of mice were harvested, manually dissected, and homogenized through a 40-μm cell strainer (pluriStrainer 40 μm, Nylon-Mesh. 43-57040-51). The samples were centrifuged for 5 min at 400 × g and resuspended in 0.5- to 1-ml PBS. All samples were stained for 15 min with the following antibodies (all from Cell Signaling Technology, Leiden, The Netherlands, Mouse Activated T Cell Markers Flow Cytometry Panel, 62447): PE CD3 (28306), violetFluor 450TM CD4 (92599), PE-Cy7 CD8α (87922). The spleen and plasma samples were incubated with 1 mL red blood cell lysis buffer for 10 min (eBioscience™ 1X RBC Lysis Buffer, 00-4333-57). After washing steps, all samples were fixed in 2% PFA. A CytoFlex S flow cytometer (Beckman Coulter, Indianapolis, IN, USA) was used for data acquisition, and data were analyzed using the CytExpert software (Beckman Coulter, Indianapolis, IN, USA) by an evaluator blinded to study groups.

3.3 Preclinical model for the investigation of the potential hidden cardiotoxicity of bempedoic acid

3.3.1 In vivo experiments

The schematic protocol for the study is shown in Figure 9. Male Wistar rats (ranging from 92 g to 150 g at the beginning of the treatment) were treated with bempedoic acid (30 mg/kg, n = 26) or its vehicle, 1% hydroxyethylcellulose (n = 61), once daily by oral gavage for 28 days. The dose of bempedoic acid was chosen based on previous studies, which showed that four weeks of treatment in rats resulted in plasma levels similar to clinical findings, while no drug-related toxicities were found (82). None of the animals died or were excluded during the treatment period. After 28 days of treatment, animals underwent echocardiography, as described previously, to determine the cardiac function of animals after chronic bempedoic acid treatment. Following the echocardiography, surgical induction of cardiac ischemia and reperfusion (I/R) was performed by occlusion of the left anterior descending coronary artery (LAD) for 30 min, followed by 120 min of reperfusion, while in one group ischemic preconditioning (IPC) was performed by three cycles of 5 min I/R prior to the index ischemia, as a positive control for cardioprotective effects in preclinical studies. Animals were

randomized into the following surgical groups: vehicle + I/R (n = 26), bempedoic acid + I/R (n = 26) and vehicle + IPC (n = 35). Animals were randomized into groups in a way that on each surgical day, at least one animal from all groups was operated on. The order of animals was randomized for each surgical day separately. For investigation of cardiac function via echocardiography, the minimum number of animals needed to be included was determined by a priori power calculation. Echocardiographic measurements were performed at the beginning of each surgical day until the sufficient number of animals were reached for both groups; however, due to the uneven distribution of BA and vehicle-treated animals, the final number of measurements is different between the two groups.

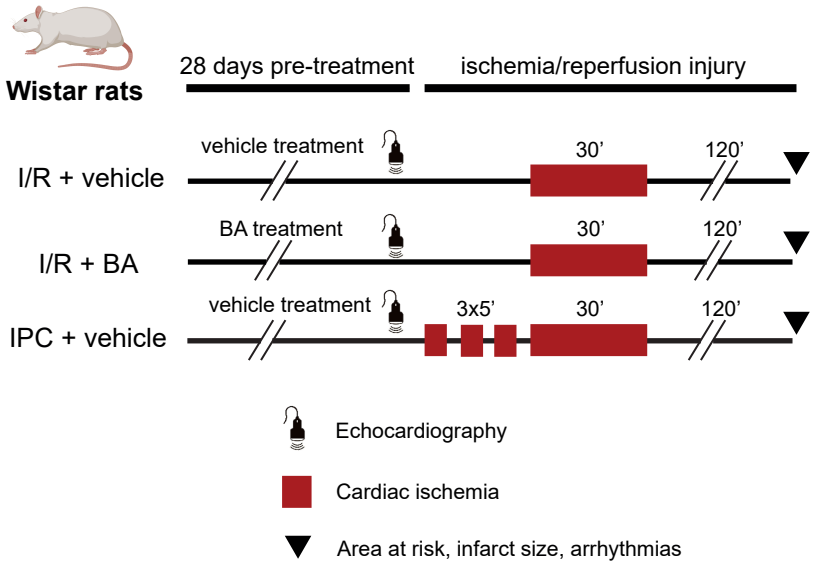

Figure 9. Schematic protocol for the rat model of acute myocardial ischemia/reperfusion injury and bempedoic acid treatment. *Adapted from Gergely et al., Int. J. Mol. Sci., 2023 (88)*

3.3.2 Induction of myocardial ischemia/reperfusion injury

Rats were anesthetized with 60 mg/kg pentobarbital intraperitoneally (i.p.) (Produlab Pharma, Raamsdonksweer, The Netherlands). The absence of pedal reflex was considered to be deep surgical anesthesia. Anesthesia was maintained by supplying half-dose pentobarbital i.p. as required when the plantar reflex could be elicited through regular paw pinch

monitoring. Body surface electrocardiogram (ECG) was monitored throughout the experiments by using standard limb leads (AD Instruments, Bella Vista, Australia). The core body temperature was maintained at physiological temperature with a heating pad (Harvard Apparatus, Holliston, MA, USA). After orotracheal intubation, rats were ventilated with a rodent ventilator (Ugo-Basile, Gemonio, Italy) with room air at a volume of 6.2 mL/kg and a frequency of 69 ± 3 breaths/min. Myocardial ischemia was induced by the occlusion of the left anterior descending coronary artery (LAD). A 5-0 Prolene suture (Ethicon, Johnson & Johnson, Budapest, Hungary) was looped around the LAD by an operator blinded to study groups. Reversible myocardial ischemia was induced by tightening a snare around the LAD. After occlusion of the LAD, the presence of myocardial ischemia was confirmed by the appearance of ST-segment changes on the ECG, I/R-induced arrhythmias, and visible pallor of the myocardial regions distal to the occlusion. After 30 minutes of LAD occlusion, 120 minutes of reperfusion was initiated by relieving the snare. Reperfusion was confirmed by ST-segment normalization and hyperaemia of the reperfused cardiac region. To prevent coagulation, the animals received i.p. injections of 100 IU/kg heparin at the 35th, 65th, and 185th minutes of experiments. Predefined exclusion criteria during surgery were the following: iatrogenic or technical error leading to the death of the animal, severe bleeding during the surgery, lack of confirmed ischemia after LAD occlusion by visual inspection or ECG alterations, lack of confirmed reperfusion after the release of the occluder by normalization of ECG alterations or visual inspection.

3.3.3 Infarct size measurement

After 120 minutes of reperfusion, hearts were excised and perfused for 2 min with oxygenated Krebs–Henseleit solution at 37 ˚C in Langendorff mode to remove blood from the tissue, LAD was re-occluded, and the area at risk (AAR) was negatively stained with Evans blue dye through the ascending aorta. For the assessment of viable myocardial tissue, 2 mm-thick slices were cut and incubated in 1% triphenyltetrazolium chloride at 37 ˚C for 14 min. The slices were weighed and scanned. Planimetric analyses were performed by two independent, blinded investigators with InfarctSize 2.4b software (Pharmahungary Group, Budapest, Hungary). Area at risk (AAR) was expressed as the proportion of the left

ventricular area, and the infarct size as the proportion of the AAR, and then the areas were normalized to the mass of each slice.

3.3.4 Arrhythmia analysis

The severity and duration of I/R-induced arrhythmias were analyzed by independent investigators in a blinded fashion. Continuous ECG records of each animal were evaluated according to the Lambeth conventions and quantified by using the 'score A' as previously described by Curtis et al. (101,102). The whole 30-minute period of ischemia and the first 15 minutes of reperfusion were quantified separately. Visual representation of the most severe arrhythmia during the 30 minutes of ischemia and the first 15 minutes of reperfusion is shown by the arrhythmia map, where the 5-minute periods were colored according to the most severe arrhythmia type.

3.4 Statistical analysis

The statistical analysis was performed using GraphPad Prism software (version 8.0.1). $p < 0.05$ was considered significant. Normal distribution of data was tested by the Shapiro–Wilk normality test. For comparisons between two groups, either a parametric two-tailed Student's t test or a nonparametric Mann–Whitney U-test was performed. Repeated measures ANOVA, followed by Bonferroni's post hoc test, was used for multiple comparisons between related groups. One-way ANOVA followed by Tukey's post hoc test or Kruskal–Wallis test followed by Dunn's post hoc test was used to compare independent groups. The post hoc tests were conducted only if F in ANOVA or Kruskal–Wallis test achieved $p < 0.05$ and there was no significant variance inhomogeneity. For correlation analysis of two continuous variables, Spearman's rho (rs) was computed, and 95% confidence intervals were obtained. ROUT analysis was performed to identify outliers, with Q value = 1%.

4 RESULTS

4.1 Investigating the mechanisms of ICI-induced cardiotoxicity

In our first study, we investigated the mechanisms of ICI-induced cardiotoxicity in mice, as described earlier. The following results have all been published in our corresponding scientific publication: (89).

4.1.1 Anti-PD-1 treatment impairs cardiac function in C57BL/6J mice

Treatment with anti-PD-1 significantly decreased left ventricular ejection fraction, while left ventricular mass and left ventricular internal diameter at systole and diastole (LVIDs and LVIDd, respectively) were significantly increased compared with the isotype control group (Figure 10/A). Diastolic function was assessed by the ratio of early diastolic filling (E, measured via pulsed-wave Doppler) and early diastolic mitral annular tissue velocity (e', measured via tissue Doppler), which correlates with the end-diastolic pressure of the left ventricle. E/e' was significantly increased after 4 weeks of anti-PD-1 treatment. Global longitudinal strain (GLS), a sensitive parameter of early cardiac dysfunction, was significantly decreased due to anti-PD1 treatment after 4 weeks of treatment. Altogether, immune checkpoint inhibition with a PD-1 inhibitor resulted in reduced cardiac systolic and diastolic function and led to left ventricular dilation in C57BL/6J mice.

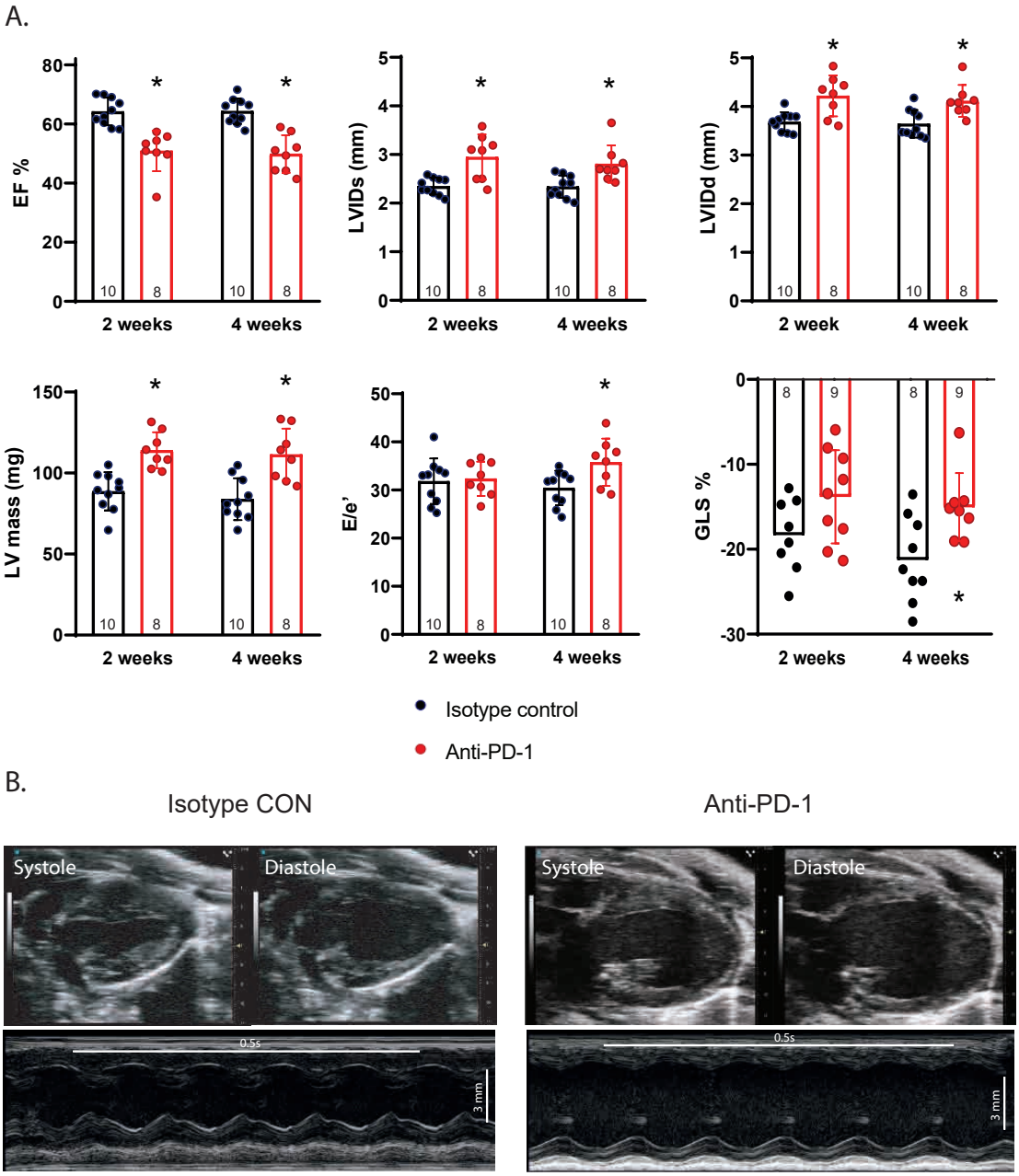

Figure 10. Impaired cardiac function following anti-PD-1 treatment assessed by transthoracic echocardiography in C57BL/6J mice. (A) Selected parameters of systolic and diastolic function are shown. EF: ejection fraction; LV mass: left ventricular mass; LVIDs: left ventricular systolic internal diameter; LVIDd: left ventricular diastolic internal diameter; GLS: global longitudinal strain. * $p < 0.05$ versus time-matched isotype control, repeated measures ANOVA, followed by Bonferroni's post hoc test, n = 8–10 per group. (B)

Representative echocardiographic B-mode and M-mode images of isotype control and anti-PD-1-treated animals. Scale bar: 3 mm. Time stamp: 0.5 s. Results are presented as mean ± standard deviation (SD). *Adapted from Gergely et al., Br. J. Pharmacol, 2023* (89)

4.1.2 Anti-PD-1 treatment does not cause cardiac fibrosis or hypertrophy

Representative histological sections of anti-PD-1-treated animals showed dilation of the ventricles (Figure 11/A), while heart weight was significantly increased compared to isotype control groups (Figure 11/B). Cardiomyocyte cross-sectional area was not altered following anti-PD-1 treatment, and microvascular density was also unaffected (Figure 11/C). Cardiac gene expression related to hypertrophy did not reveal significant changes after anti-PD-1 treatment (Figure 11/E), whereas a mild tendency towards increased cardiac fibrosis was seen, measured by either Sirius red staining (Figure 11/D) or gene expression of fibrosis markers by qRT-PCR (Figure 11/F). Overall, anti-PD-1 treatment did not affect cardiac hypertrophy and fibrosis significantly. Thus, distinct mechanisms may play a role in the previously observed anti-PD-1-induced cardiac dysfunction and left ventricular dilation.

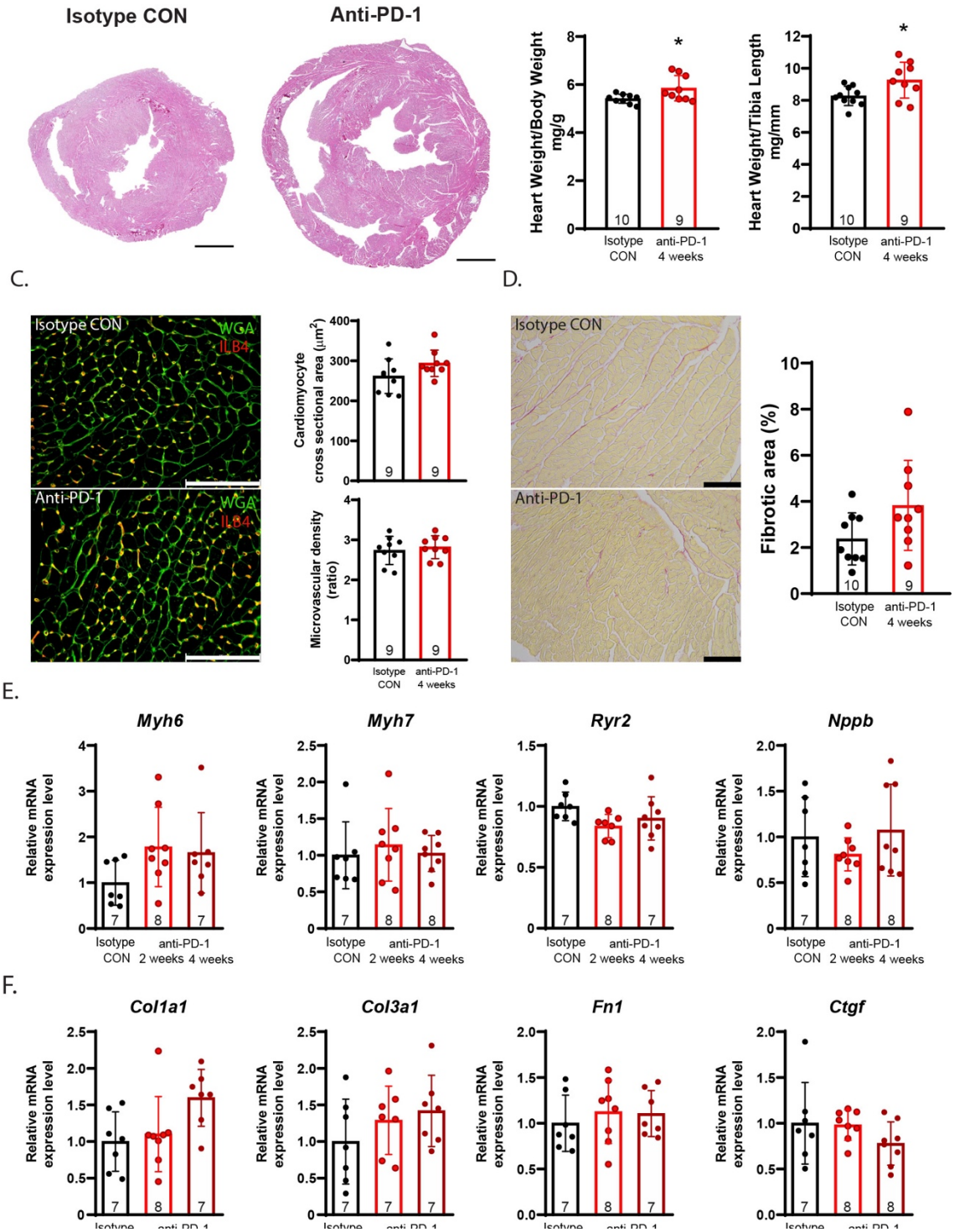

Figure 11. Concentric hypertrophy of the heart or cardiac fibrosis was not seen following anti-PD-1 treatment. (A) Representative images of hematoxylin and eosin-stained hearts of isotype control and anti-PD-1-treated animals. Scale bar: 1 mm. (B)

Comparison of heart weights relative to the body weight or tibia length of the animals. * $p <$ 0.05 vs Isotype CON, Student's t-test, n = 9-10 / group. (C) Cardiomyocyte cross-sectional area (CSA) was determined on WGA-stained sections (representative images are shown). Microvascular density was determined by the ratio of the microvascular number (stained with ILB4) and CSA. Scale bar: 100 μm. Student's t-test: n.s., n = 9-10 / group. (D) Representative images are shown of hearts stained with Sirius red following anti-PD-1 treatment. Cardiac fibrosis is expressed as the ratio between the stained area and the total area of the slice. Student's t-test: n.s., n = 9-10 / group. Scale bar: 100 μm. (E), (F) qRT-PCR was performed to assess relative expression of hypertrophy- (E) and fibrosis-related (F) genes. One-way ANOVA or Kruskal-Wallis test was performed, followed by Tukey's or Dunn's post hoc test if the test's p value was significant, n = 7-8 / group. Results are presented as mean ± standard deviation (SD). Exact group sizes are shown in each graph. *Adapted from Gergely et al., Br. J. Pharmacol, 2023* (89)

4.1.3 Anti-PD-1 treatment leads to transcriptomic changes in the heart

To investigate the underlying mechanisms of ICI-induced cardiac dysfunction, we characterized the transcriptomic changes occurring after anti-PD-1 treatment in the heart with bulk RNA sequencing. After 2 weeks of PD-1 inhibitor therapy, 538 genes were differentially expressed after multiple comparison corrections, compared to isotype control treatment. Of these, 266 were upregulated and 272 were downregulated. After 4 weeks of PD-1 inhibitor therapy, 55 genes were differentially expressed, with 17 being upregulated and 38 downregulated (Figure 12/A). Figure 12/B shows the 50 most significantly changed genes.

Furthermore, to analyze the functional changes after PD-1 inhibition, we have performed Gene Ontology (GO) analysis. After 2 weeks of treatment, several GO terms related to cardiac contractile function were downregulated, while GO terms indicating metabolic changes were upregulated. After 4 weeks, upregulated genes with the highest fold enrichment were related to antigen presentation via major histocompatibility complex (MHC) molecules (Figure 13).

Altogether, these findings indicate that immune checkpoint inhibition with anti-PD-1 treatment leads to a distinct transcriptomic profile, characterized by reduced cardiac

contractility, metabolic changes, and increased antigen presentation.

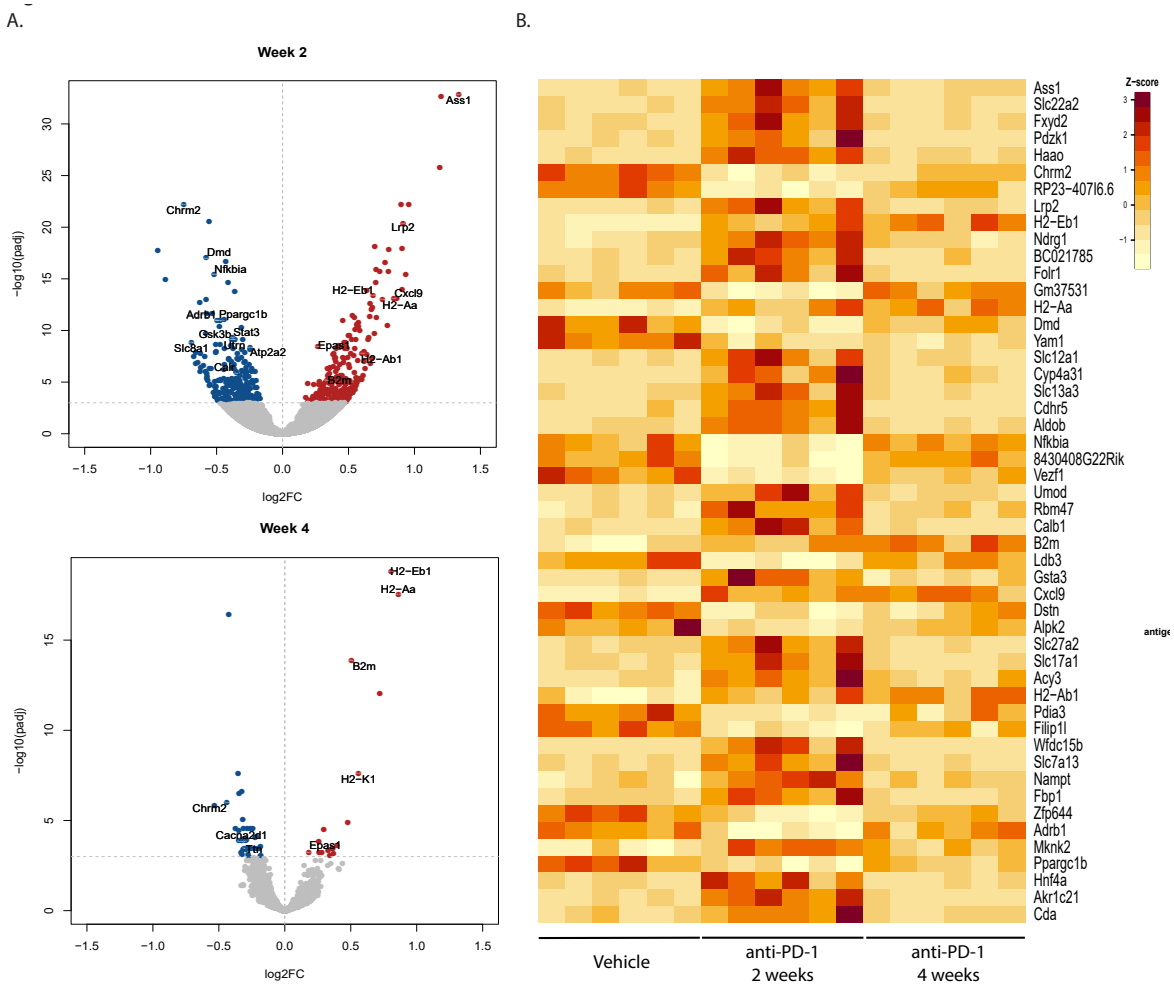

Figure 12. RNA sequencing shows a distinct myocardial transcriptomic profile after anti-PD-1 treatment in C57BL/6J mice. (A) Volcano plots showing down- and upregulated genes after 2 and 4 weeks of anti-PD-1 treatment. (B) Heat map showing gene-wise Z-scores of the normalized read counts of the 50 most significant differentially expressed genes after 2 and 4 weeks of anti-PD-1 treatment. *n* = 6 animals / group. *Adapted from Gergely et al., Br. J. Pharmacol, 2023* (89)

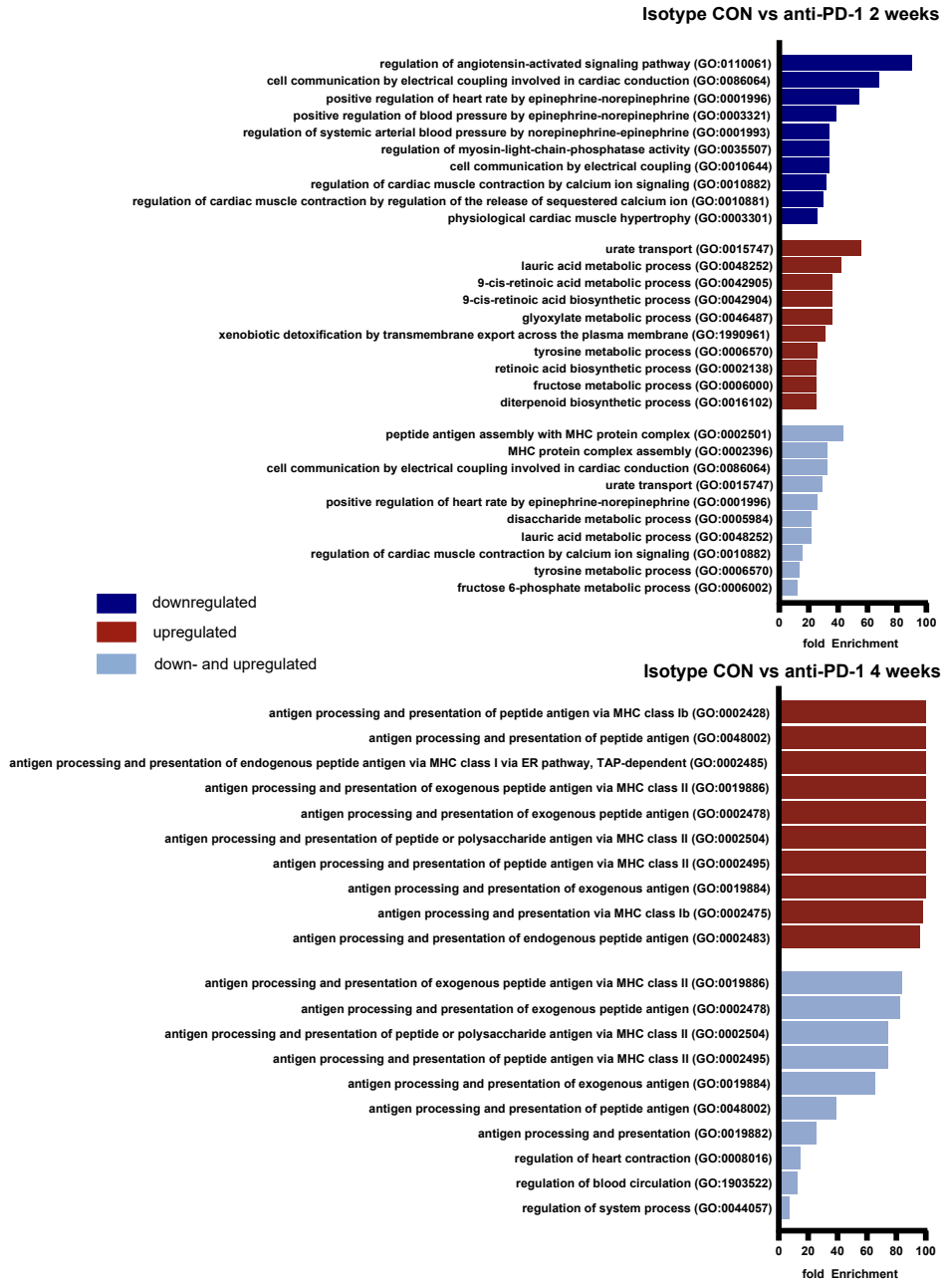

Figure 13. Gene Ontology (GO) biological process enrichment analysis of the differentially expressed transcripts following 2 and 4 weeks of anti-PD-1 treatment, compared to isotype control. GO terms were categorized based on their expression pattern (downregulated, upregulated, down- and upregulated). The top 10 GO terms with the highest fold enrichment values are shown in each category. All of the shown GO terms had adjusted

p values < 0.05 and were considered significant. *n* = 6 animals / group. *Adapted from Gergely et al., Br. J. Pharmacol, 2023 (89)*

4.1.4 Anti-PD-1 treatment leads to immune activation in the thymus

To investigate the potential pro-inflammatory effects of anti-PD-1 treatment in the development of cardiac dysfunction, we have measured the changes in inflammatory gene expression locally (in the heart) and remotely (in the thymus and spleen) via qRT-PCR (Figure 14). Anti-PD-1 treatment significantly increased the expression of *Il1b* in the heart after 2 weeks, while *Aif1* and *Cd163* - markers of different macrophage populations - were increased after 4 weeks of PD-1 inhibitor treatment. However, other cytokines, or cell-type specific markers of inflammation were not affected significantly, including *Cd3e* expression (Figure 14/A). Furthermore, CD3ε immunohistochemistry did not show an increase in $CD3^+$ T cells in the myocardium (Figure 14/B).

Immune checkpoint inhibition has also been reported to cause various systemic immune-related adverse effects, whereas thymus alterations are associated with ICI myocarditis development (59). After anti-PD-1 treatment, we observed increased gene expression of pro-inflammatory cytokines in the thymus (*Il3, Il6, Il17a, Il17f, Il23*) (Figure 14/C). Of these, *Il17a* showed the highest increase compared to the isotype control-treated group. Importantly, gene expression of the anti-inflammatory cytokine *Il10* did not change significantly, leading to an increased *Il17a*/*Il10* ratio after anti-PD-1 treatment. Furthermore, we also assessed inflammatory changes in the spleen, where only *Ifng* showed increased expression after 2 weeks of anti-PD-1 treatment (Figure 14/D).

Altogether, these findings indicate that cardiac dysfunction after anti-PD-1 treatment in healthy C57BL/6J mice can develop independently of significant T cell infiltration into the myocardium. However, gene expression of pro-inflammatory cytokines is markedly increased in the thymus, suggesting thymus alterations and remote cytokine production as a potential mediator of ICI-induced cardiac dysfunction.

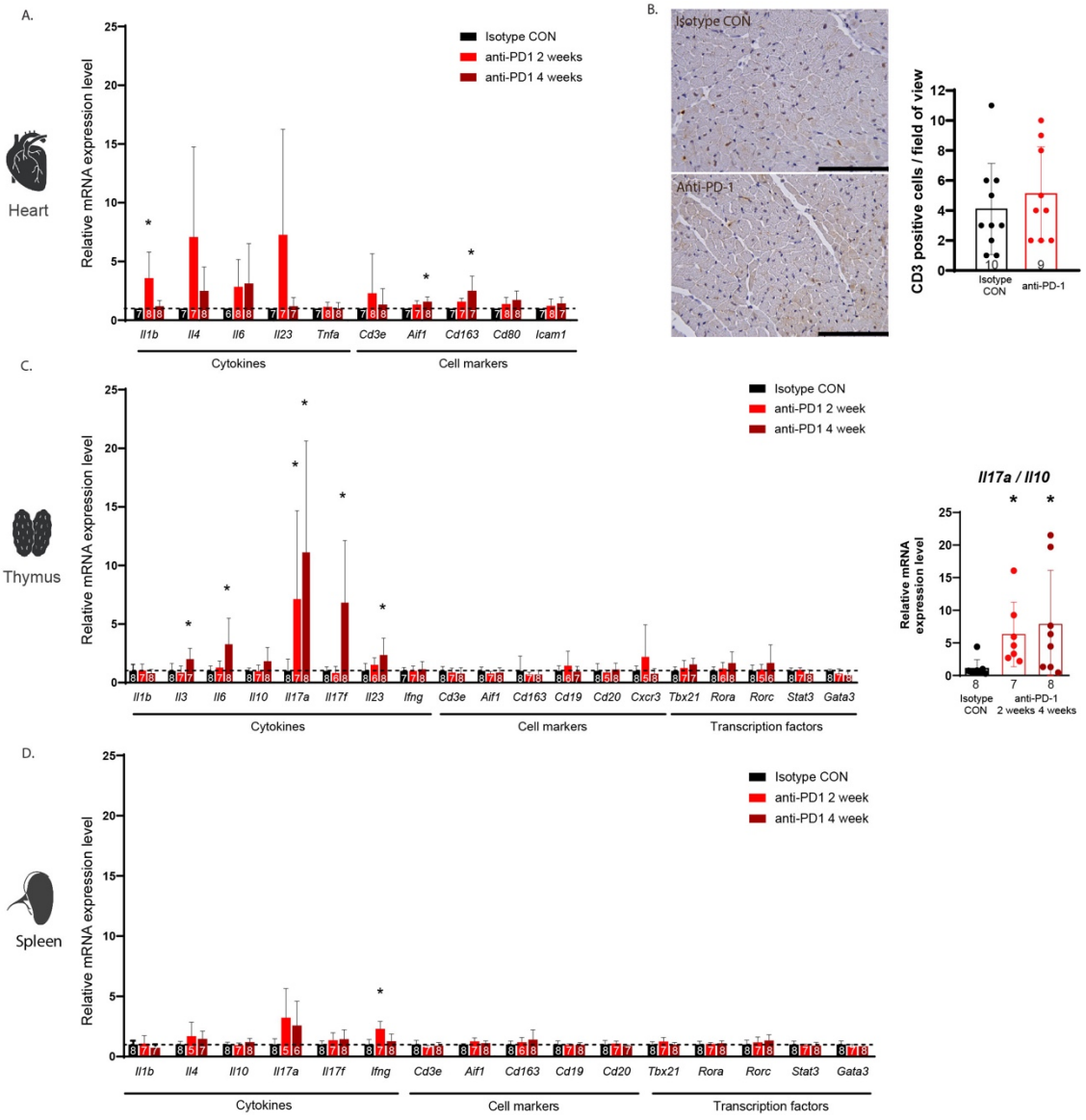

Figure 14. Anti-PD-1 treatment causes mild inflammation in the heart and prominent inflammatory gene expression in the thymus of C57BL/6J mice. (A) Analysis of mRNA expression of cytokines (Il1b, Il4, Il6, Il23, Tnfa) and cell markers (Cd3e, Aif1, Cd163, Cd80, Icam1) in the heart by qRT-PCR. * $p < 0.05$ vs Isotype CON, one-way ANOVA followed by Tukey's post hoc test, n = 6-8 / group (B) Representative images and quantification of CD3ε immunohistochemistry after anti-PD-1 treatment. Scale bar: 100 µm. Student's t-test: n.s., n = 9-10 / group. (C) Analysis of mRNA expression of cytokines (Il1b, Il3, Il6, Il10, Il17a, Il17f, Il23, Ifng), cell markers (Cd3e, Aif1, Cd163, Cd19, Cd20, Cxcr3) and transcription

factors (Tbx21, Rora, Rorc, Stat3, Gata3) in the thymus by qRT-PCR. * $p < 0.05$ vs Isotype CON, one-way ANOVA followed by Tukey's post hoc test, $n = 6$-8 / group. (D) Analysis of mRNA expression of cytokines (Il1b, Il4, Il6, Il10, Il17a, Il17f, Ifng), cell markers (Cd3e, Aif1, Cd163, Cd19, Cd20) and transcription factors (Tbx21, Rora, Rorc, Stat3, Gata3) in the spleen by qRT-PCR. * $p < 0.05$ vs Isotype CON, one-way ANOVA followed by Tukey's post hoc test, $n = 6$-8 / group. Results are presented as mean ± standard deviation (SD). Exact group sizes are shown in each graph. *Adapted from Gergely et al., Br. J. Pharmacol, 2023* (89)

4.1.5 Anti-PD-1 does not cause cardiac dysfunction in BALB/c mice and leads to more balanced cytokine expression in the thymus

Following the findings that anti-PD-1 treatment induced pro-inflammatory gene expression in the thymus, we investigated the effects of PD-1 inhibition in BALB/c mice, a mouse strain known to differ in systemic T cell-mediated immune response, mainly exhibiting Th2-type immune response (103). As we have seen the most prominent changes in cardiac gene expression after 2 weeks of treatment in C57BL/6J mice, we have treated BALB/c mice for 2 weeks with isotype control or anti-PD-1 (Figure 8/B). In contrast to C57BL/6J mice, BALB/c mice did not show increased heart weight, left ventricular dilation, or cardiac dysfunction following PD-1 inhibition (Figure 15/A, B, C), suggesting that this strain of mice is resistant to anti-PD-1-induced cardiac dysfunction in this experimental setting. Moreover, we investigated inflammatory changes in BALB/c mice. In the heart, the expression of *Il4* and *Cd163* increased significantly, while in contrast to C57BL/6J mice, *Il1b* expression was not altered (Figure 16/A). In the thymus, we have seen a prominent response to anti-PD-1 treatment, with the increase of *Il3*, *Il6*, *Il10*, *Il17a*, *Il17f*, *Il23*, *Rora*, and a decrease of *Il4* and *Gata3*. Interestingly, as opposed to C57BL/6J mice, the expression of anti-inflammatory cytokine *Il10* was significantly increased, leading to a lower ratio of *Il17a/Il10* (Figure 16/B).

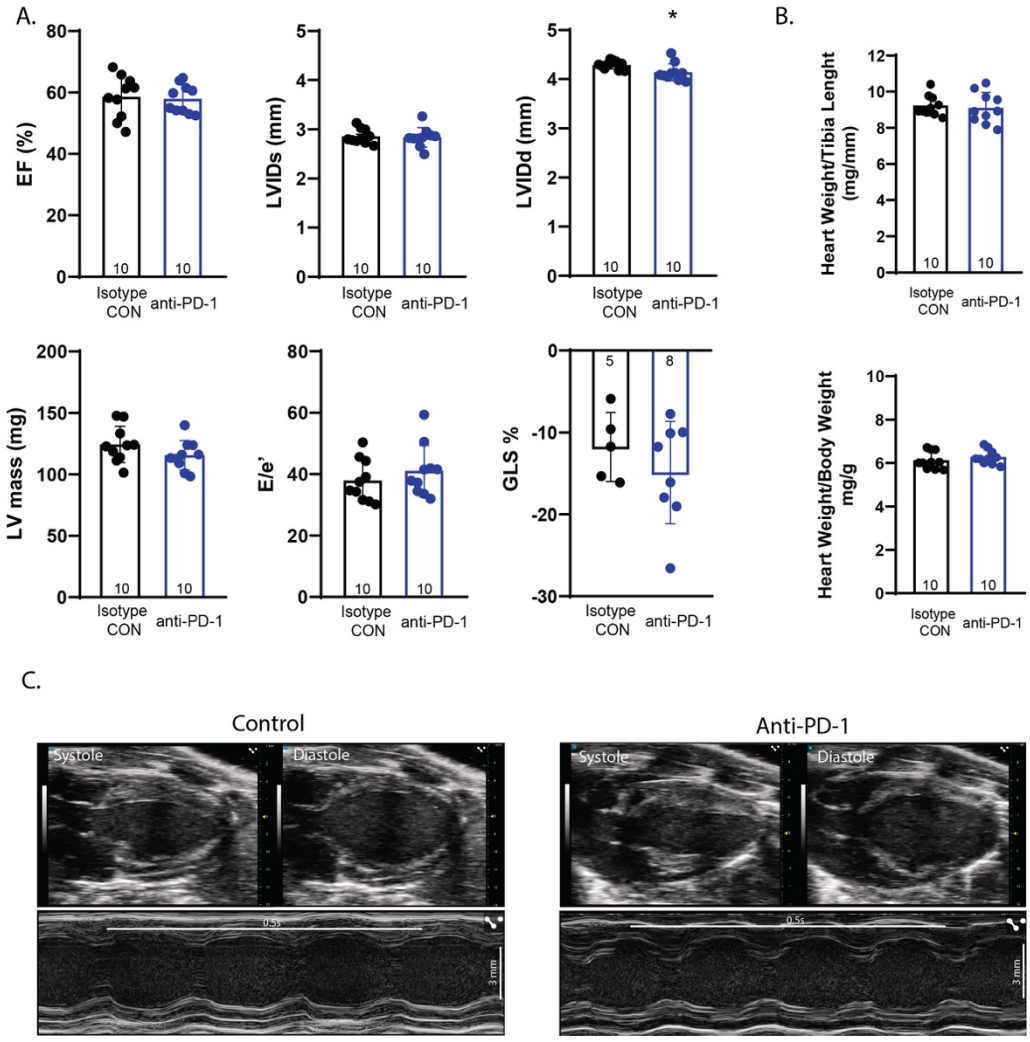

Figure 15. Anti-PD-1 treatment does not cause cardiac dysfunction or left ventricular dilation in BALB/c mice. (A) Selected parameters of systolic and diastolic function are shown. EF: ejection fraction; LV mass: left ventricular mass; LVIDs: left ventricular systolic internal diameter; LVIDd: left ventricular diastolic internal diameter; GLS: global longitudinal strain. * $p < 0.05$, vs isotype control, Student's two-tailed t-test, $n = 10$ / group for quantification of EF, LVIDs, LVIDd, LV mass, E/e', $n = 5$-8 / group for quantification of GLS. (B) Comparison of heart weights relative to the body weight or tibia length of the animals. * $p < 0.05$ vs Isotype CON, Student's t-test, $n = 10$ / group. (C) Representative echocardiographic B-mode and M-mode images of isotype control and anti-PD-1-treated animals. Scale bar: 3 mm. Time stamp: 0.5s. Results are presented as mean ± standard

deviation (SD). Exact group sizes are shown in each graph. *Adapted from Gergely et al., Br. J. Pharmacol, 2023* (89)

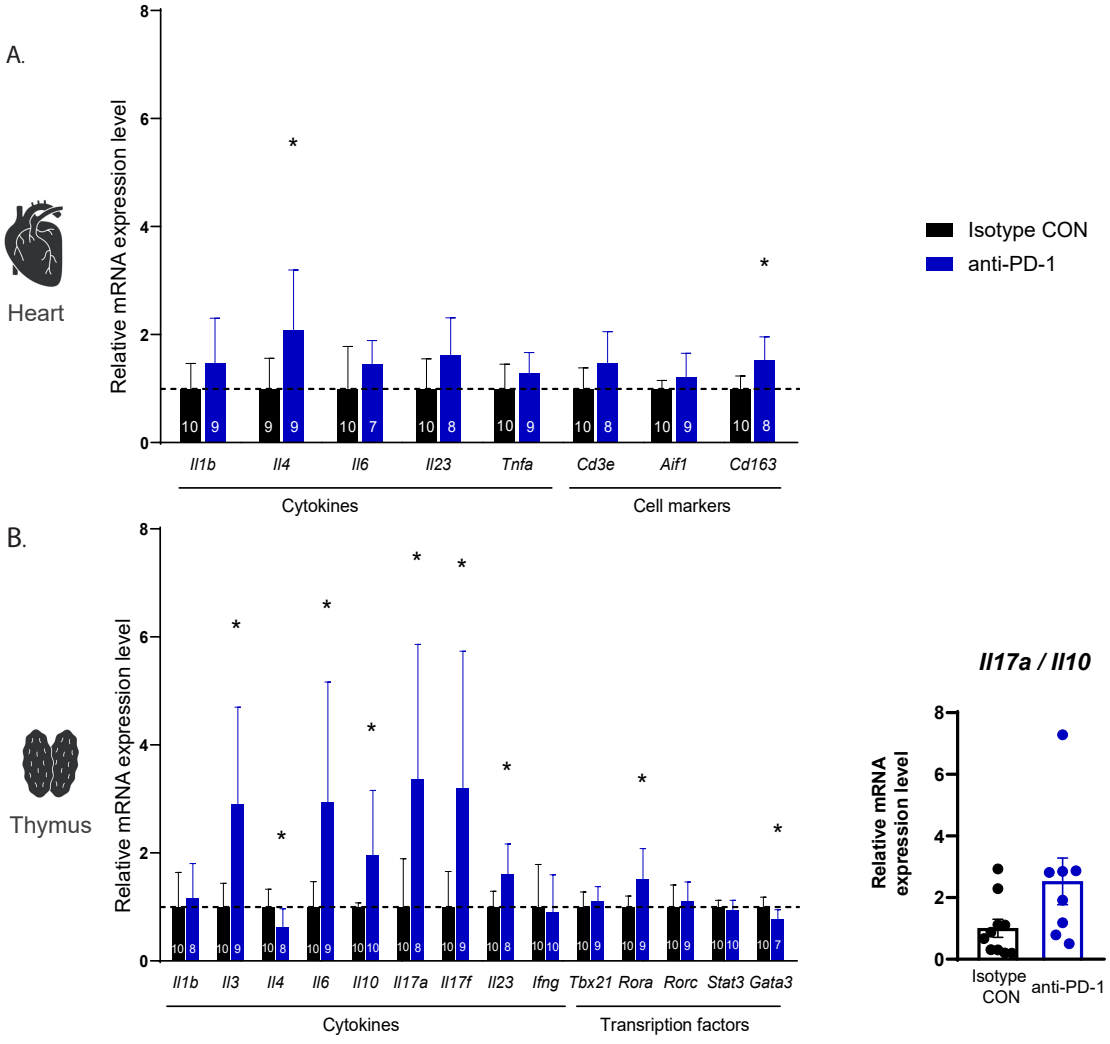

Figure 16. Investigation of anti-PD-1 induced inflammatory changes in BALB/c mice. (A) Analysis of mRNA expression of cytokines (Il1b, Il4, Il6, Il23, Tnfa) and cell markers (Cd3e, Aif1, Cd163, Cd80, Icam1) in the heart by qRT-PCR. * $p < 0.05$ vs Isotype CON, Student's t-test, n = 7-10 / group. (B) Analysis of mRNA expression of cytokines (Il1b, Il3, Il6, Il10, Il17a, Il17f, Il23, Ifng), cell markers (Cd3e, Aif1, Cd163, Cd19, Cd20, Cxcr3) and transcription factors (Tbx21, Rora, Rorc, Stat3, Gata3) in the thymus by qRT-PCR. * $p <$

0.05 vs Isotype CON, Student's t-test, n = 7-10 / group. Results are presented as mean ± standard deviation (SD). Exact group sizes are shown in each graph. *Adapted from Gergely et al., Br. J. Pharmacol, 2023* (89)

4.1.6 Anti-IL17A treatment or CD4 T cell depletion prevents the development of anti-PD-1 induced cardiac dysfunction

After the molecular characterization of ICI-induced cardiac dysfunction, we aimed to further investigate mechanisms that could be targeted pharmacologically to alleviate anti-PD-1-induced cardiotoxicity. Our previous results showed that the expression of several pro-inflammatory cytokines increased after anti-PD-1 treatment. Thus, first we aimed to deplete $CD4^+$ T cells, major contributors to cytokine production. As expression of *Il17a* was most prominently induced by PD-1 inhibition, we also targeted IL-17A with a monoclonal antibody, as a clinically relevant intervention (Figure 8/C). We have found that both depletion of $CD4^+$ T cells and selective blockade of IL-17A prevented the development of ICI-induced cardiac dysfunction, as shown by maintained EF in the respective groups, while EF was decreased with anti-PD-1 treatment alone (Figure 17/A, B). The efficacy of CD4 depletion was confirmed by flow cytometry in the spleen and thymus (Figure 17/C). Interestingly, treatment with anti-PD-1 antibody alone, or in combination with anti-IL17A, has also modestly decreased the $CD4^+$ T cell population in the spleen (Figure 17/C).

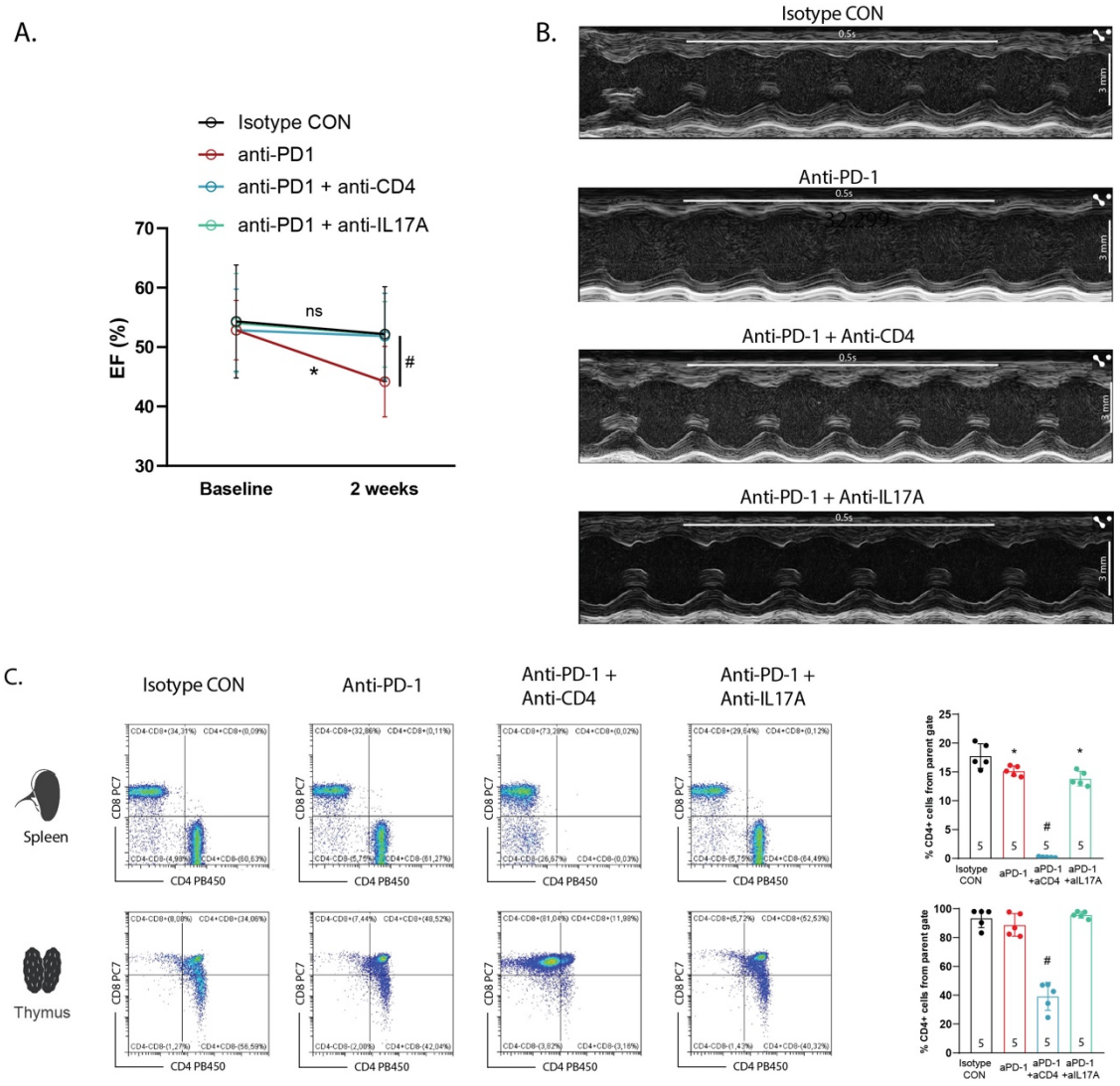

Figure 17. Anti-PD-1-induced cardiac dysfunction is prevented by co-treatment with anti-CD4 or anti-IL17A antibody. (A) Treatment with anti-CD4 or anti-IL17A prevented the decline in ejection fraction seen with anti-PD-1 treatment alone. * $p < 0.05$ vs corresponding baseline, repeated measures ANOVA, followed by Bonferroni's post hoc test. # $p < 0.05$ vs. anti-PD-1 at 2 weeks, repeated measures ANOVA, followed by Dunnett's post hoc test, $n = 9$ for isotype CON group, $n = 10$ for anti-PD-1, anti-PD-1+anti-CD4, anti-PD-1+anti-IL17A groups. Results are presented as mean ± standard deviation (SD). (C) Representative echocardiographic M-mode images of isotype control, anti-PD-1, anti-PD-1+anti-CD4, and anti-PD-1+anti-IL17A treated animals. Scale bar: 3 mm. Time stamp: 0.5s. (D) Representative flow cytometry images and quantification of CD4+ cells in the spleen and

thymus of isotype control, anti-PD-1, anti-PD-1+anti-CD4, and anti-PD-1+anti-IL17A treated animals. * $p < 0.05$ vs isotype CON, one-way ANOVA, followed by Tukey's post hoc test. # $p < 0.05$ vs isotype CON, anti-PD-1 and anti-PD-1+anti-IL17A groups, one-way ANOVA, followed by Tukey's post hoc test, $n = 5$ / group. Results are presented as mean ± standard deviation (SD). *Adapted from Gergely et al., Br. J. Pharmacol, 2023* (89)

4.2 Investigating bempedoic acid for potential hidden cardiotoxicity

In our second study, we investigated the effects of bempedoic acid on cardiac ischemia/reperfusion injury and its potential hidden cardiotoxic effects. The following results have all been published in our corresponding scientific publication (88).

4.2.1 Bempedoic acid treatment did not affect cardiac function or morphology in healthy animals

After 28 days of treatment with bempedoic acid, echocardiography was performed to investigate the effect of chronic bempedoic acid treatment on cardiac functional and morphological parameters. Bempedoic acid did not affect systolic or diastolic function, as shown by normal ejection fraction, fractional shortening, and similar E/e' ratios, respectively (Figure 18). Moreover, bempedoic acid did not alter the left ventricular diameters or the total mass of the ventricle. In summary, these data show that the use of bempedoic acid does not affect cardiac function or morphology in healthy animals.

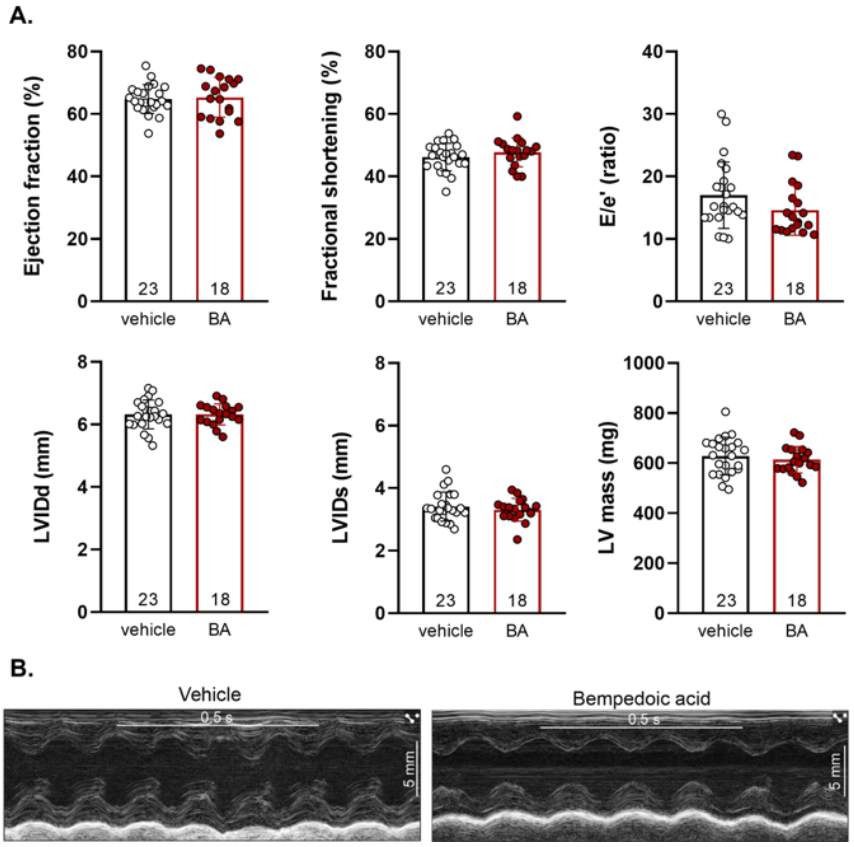

Figure 18. Cardiac function after vehicle or BA treatment. (**A**) Selected parameters of systolic and diastolic function are shown. Statistics: Student's two-tailed t-test or Mann–Whitney U-test: n.s., n = 18 for BA and n = 23 for vehicle-treated groups. Results are presented as means ± SD. (**B**) Representative echocardiographic M-mode images of vehicle and BA-treated animals. Scale bar: 5 mm. Time stamp: 0.5 s. BA: bempedoic acid. EF: ejection fraction. FS: fractional shortening. E/e': ratio between peak Doppler blood inflow velocity across the mitral valve during early diastole and peak tissue Doppler of myocardial relaxation velocity at the mitral valve annulus during early diastole. LVIDd: left ventricular internal diameter at diastole. LVIDs: left ventricular internal diameter at systole. LV mass: left ventricular mass. *Adapted from Gergely et al., Int. J. Mol. Sci., 2023* (88).

4.2.2 Bempedoic acid pretreatment did not alter infarct size or mortality after ischemia/reperfusion injury

To investigate the potential hidden cardiotoxic effects of bempedoic acid, we have induced cardiac ischemia/reperfusion injury, as described previously. No statistically significant difference was found between groups in mortality during I/R surgery (I/R + vehicle: 19.23%, I/R + BA: 29.17%, IPC + BA: 10%, Chi-square test: n.s., n = 26–30/group). In the I/R + vehicle group, out of the 26 performed surgeries, 0 had to be excluded, 21 animals survived the surgery, and five died. In the I/R + BA group, out of the 26 performed surgeries, two had to be excluded due to predefined exclusion criteria, 17 animals survived, and seven animals died. In the IPC + vehicle group, out of the 35 performed surgeries, seven had to be excluded, 27 survived, and three animals died. Altogether, this suggests that bempedoic acid pretreatment does not exacerbate nor protect from I/R-induced acute mortality in this model. Next, we measured myocardial infarct size, expressed as a proportion of the total LV area exposed to ischemia (area at risk, AAR). The AARs did not differ between groups (I/R + vehicle: 29.61% ± 3.08, I/R + BA: 33.90% ± 1.95, IPC + vehicle: 27.29% ± 2.30, Kruskal–Wallis test: n.s., n = 11-15/group). Chronic pretreatment with BA did not influence infarct size compared to the vehicle group, showing no hidden cardiotoxic (nor cardioprotective) effects, while the positive control for cardioprotective effects, IPC, significantly reduced it (Figure 19).

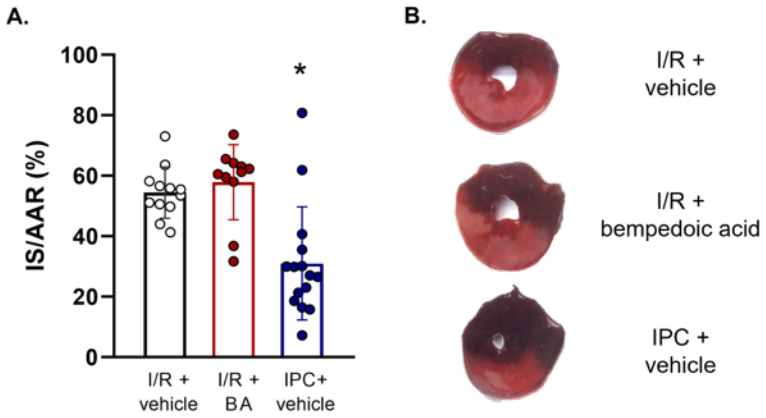

Figure 19. Myocardial infarct sizes. (**A**) * $p < 0.05$ vs I/R + vehicle and I/R + BA groups, Kruskal–Wallis test, followed by Dunn's post hoc test, n = 11–15 / group. Results are presented as means ± SD. (**B**) Representative triphenyltetrazolium-chloride-stained slices. BA: bempedoic acid. IS: infarct size. AAR: area at risk. IPC: ischemic preconditioning. I/R: ischemia/reperfusion. *Adapted from Gergely et al., Int. J. Mol. Sci., 2023* (88).

4.2.3 Bempedoic acid pretreatment decreased reperfusion-induced arrhythmias

Arrhythmias were analyzed by arrhythmia scoring, as described previously, and visualized using arrhythmia maps (Figure 20). The arrhythmia score during ischemia was not affected by bempedoic acid compared to vehicle vehicle-treated group, while IPC significantly decreased it. However, during reperfusion, the arrhythmia score was significantly reduced both by bempedoic acid treatment and IPC, compared to the I/R + vehicle group (Figure 21). The decrease in arrhythmia score during reperfusion by bempedoic acid can be attributed to the reduction in the incidence of non-sustained ventricular tachycardias (NSVTs). In summary, bempedoic did not show hidden cardiotoxic properties in terms of arrhythmia induction, in contrast, a mild decrease in reperfusion-induced arrhythmias was observed.

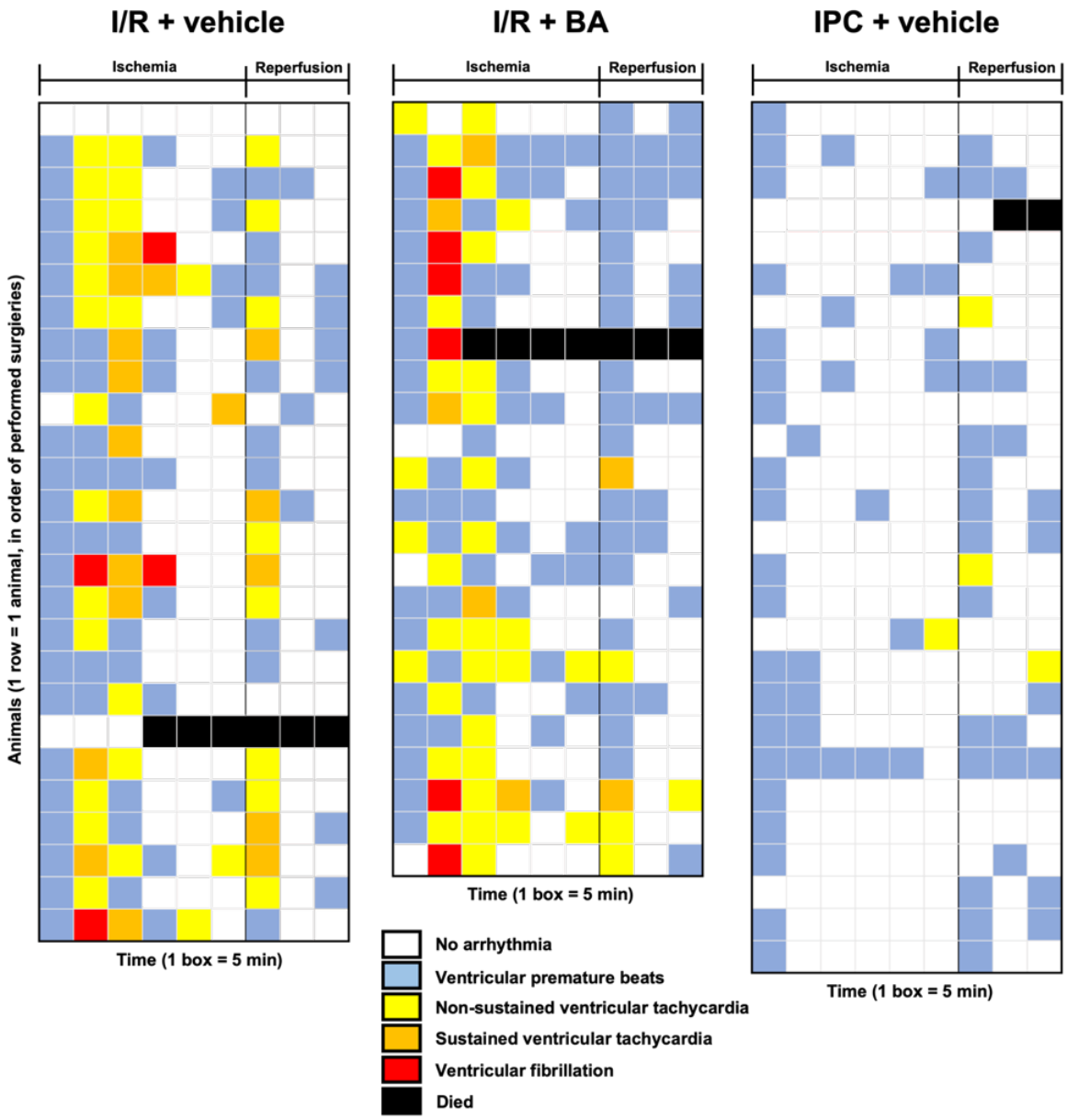

Figure 20. Arrhythmia maps. The most severe arrhythmia is shown in 5-minute intervals during the 30 minutes of ischemia and at the first 15 minutes of reperfusion, in the order of performed surgeries. Each row represents arrhythmias of one animal. Each box shows 5-minute periods colored according to the most severe arrhythmia. Animals that died during IPC (n = 1) are not shown on the arrhythmia map. BA: bempedoic acid. I/R: ischemia/reperfusion. IPC: ischemic preconditioning. *Adapted from Gergely et al., Int. J. Mol. Sci., 2023* (88).

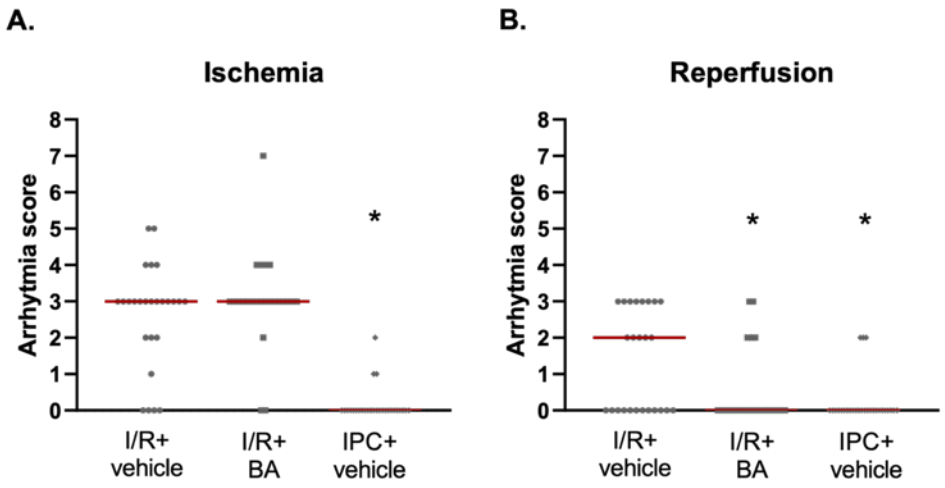

Figure 21. Arrhythmia scores during ischemia (**A**) and the first 15 min of reperfusion (**B**). * $p < 0.05$ vs. I/R + vehicle group, Kruskal–Wallis test, followed by Dunn's post hoc test, n = 23–27/group. Results are presented as median (red line) with individual data points. BA: bempedoic acid. IPC: ischemic preconditioning. I/R: ischemia/reperfusion. *Adapted from Gergely et al., Int. J. Mol. Sci., 2023* (88).

5 DISCUSSION

Here, we investigated two emerging topics in the field of drug-induced cardiotoxicity: (1) the mechanism of cardiotoxicity induced by an anti-PD-1 immune checkpoint inhibitor (a novel anti-cancer immunotherapeutic monoclonal antibody), and (2) the testing of hidden cardiotoxicity of bempedoic acid, a novel antihyperlipidemic medication. In our first study, we have shown that treatment with anti-PD-1 monoclonal antibody induced cardiac dysfunction in mice, with mechanisms related to thymus-derived IL-17A signaling, suggesting that inhibition of the pro-inflammatory IL-17A cytokine could be a cardioprotective strategy to alleviate ICI-induced cardiac dysfunction. In our second study, hidden cardiotoxic properties of bempedoic acid were not observed in a rat model of acute myocardial ischemia/reperfusion injury, suggesting its safe application in patients with ischemic heart diseases.

5.1 Cardio-oncology: mechanism of immune checkpoint inhibitor-induced cardiac dysfunction

As the use of immune checkpoint inhibitors is rapidly rising (104), a broad spectrum of cardiovascular adverse effects is being recognized, among the firstly discovered ICI-induced myocarditis. Cardiac dysfunction or heart failure after ICI therapy without concomitant myocarditis is one of the six direct cardiac toxicities highlighted by the 2022 European Society of Cardiology Guidelines on Cardio-oncology, termed as “non-inflammatory heart failure” (60). In clinical studies, the presence of cardiac dysfunction or heart failure after ICI treatment varies (53) depending on the study design. Heart failure has been identified as a late-onset adverse event in a pharmacovigilance study (52), while in a Danish nationwide study increased risk of heart failure development was seen after 6 months of treatment in lung cancer patients (47). In a large meta-analysis of 48 randomized controlled trials, increased odds of heart failure were seen in patients with ICI use (105). Moreover, in a single-center retrospective study, the majority (69.6%) of major adverse cardiac events occurring with ICI use were attributed to heart failure (106). While the incidence of cardiac dysfunction

or heart failure is increasingly recognized after ICI treatment, little is known about the potential mechanisms.

The interaction between the tumour and the immune system may influence the response to ICI therapy, possibly affecting cardiac adverse events. In a preclinical study, anti-PD-1 treatment of only B16-F10 melanoma-bearing BALB/c mice caused decreased cardiac function and inflammation in the heart, while non-tumour-bearing animals exhibited normal cardiac function (107). Similar findings were seen in another study, where only tumour-bearing C57BL/6 mice exhibited cardiac dysfunction after anti-PD-1 therapy (51). Nevertheless, genetic deletion of PD-1 in the BALB/c background led to dilated cardiomyopathy (108) (with autoantibody development against cardiac troponins (109)), without tumour presence, suggesting that while cancer may be a modulating factor, it is not necessary for the development of cardiac effects after immune checkpoint inhibition. Clinically, tumour-free cancer patients (e.g., after complete resection) treated with adjuvant ICI therapy to prevent recurrence (110) may still be at risk for cardiovascular adverse events.

In bulk RNA sequencing, anti-PD-1 treatment resulted in a distinct transcriptomic profile, including mild inflammatory changes, as well as disruption of cardiac contractile processes and antigen presentation, as shown by Gene Ontology Enrichment analysis. Out of the differentially expressed genes, inflammatory pathways were altered by anti-PD-1 treatment, albeit only to a modest degree. Of note, *Cxcl9,* encoding the pro-inflammatory chemokine (C-X-C motif) ligand 9 (CXCL9), was upregulated in the myocardium. CXCL9 binds to CXCR3, which interaction is responsible for inducing chemotaxis and leukocyte extravasation. Recently, the CXCR3-CXCL9 axis has been implicated in ICI-myocarditis as an important mediator of the T cell–macrophage cross-talk and as a potential therapeutic target (111,112). Moreover, CXCR3-CXCL9 signaling has been shown to play a role in heart failure development, as CXCR3 deficiency improved pressure-overload induced heart failure in mice by inhibition of myocardial T cell infiltration (113,114), whereas in heart failure patients, circulating CXCL9 levels have been associated with disease severity (115). Moreover, in a clinical study, increased serum levels of CXCL9 have been observed in patients with immune-related adverse events after ICI therapy compared to patients without

adverse events (114). These findings suggest that CXCL9 may be one of the mediators behind the cardiac effects of anti-PD-1 treatment.

Despite the mild inflammatory changes in the heart, we did not observe significant T cell infiltration into the myocardium, thus, we sought to investigate systemic inflammatory changes after ICI therapy as further potential mediators of the cardiac adverse effects. Alterations of the thymus have been recently associated with ICI-myocarditis (59). Compared to other tumour types, thymic epithelial tumors were more commonly associated with ICI-related adverse effects and presented with increased severity (59,116). Moreover, morphological characteristics of the thymus (assessed via CT scan) or the presence of anti-acetylcholine-receptor antibodies (a surrogate for thymus activity) were also associated with ICI myocarditis development (59), while in a case report, thymus hyperplasia has been observed in patients after ICI treatment (117). Altogether, these findings suggest a central role for the thymus in mediating ICI-related adverse events, including cardiovascular toxicity. Nevertheless, the molecular mechanisms occurring in the thymus during ICI treatment are unknown. In our study, gene expression of several pro-inflammatory cytokines was upregulated in the thymus after anti-PD-1 treatment, including *Il3*, *Il6*, *Il17a*, *Il17f,* and *Il23*, with *Il17a* showing the most prominent upregulation. IL-17 has been associated with ICI treatment previously: in human peripheral blood cells, anti-PD-1 treatment increased IL-17 production *in vitro* (118). Moreover, the level of circulating IL-17 correlated with ICI-induced colitis (119), while increased Th17 subpopulations were associated with autoimmune toxicities after ICI therapy (120). Regarding cardiac effects, in previous studies, IL-17A was associated with left ventricular dilation and cardiac dysfunction in an experimental autoimmune myocarditis model (121). In mice with pressure overload-induced heart failure, anti-CTLA-4 treatment led to exacerbated cardiac dysfunction mediated by Th17 cell differentiation, while inhibition of IL-17 with monoclonal antibodies ameliorated the anti-CTLA-4-mediated adverse cardiac effects in this heart failure model (122). Moreover, elevated IL-17 serum levels were associated with heart failure severity in clinical studies (123,124), whereas circulating IL-17 levels were increased in mice with pressure overload-induced heart failure as well, and IL-17 deficiency improved cardiac function (125).

To further investigate the role of systemic inflammatory changes in the cardiac effects of anti-PD-1 treatment, we have utilized BALB/c mice, a strain with a markedly different, Th2-dominant immune response, as opposed to the predominant Th1-type immune response in C57BL/6J mice (126). Here, we have found that cardiac dysfunction and left ventricular dilation were not evident in BALB/c mice after anti-PD-1 treatment, whereas in the thymus of the animals, *Il10* (encoding the anti-inflammatory cytokine IL-10) was also upregulated, leading to a more balanced IL-17A / IL-10 ratio. To test whether pro-inflammatory cytokine production, and specifically IL-17A, could be utilized as a therapeutic target to alleviate ICI-induced cardiac dysfunction, we co-administered CD4-depleting or IL-17A neutralizing antibodies with anti-PD-1 treatment in C57BL/6J mice. Here, we have found that both interventions prevented the cardiac decline seen with anti-PD-1 treatment alone. IL-17 neutralizing monoclonal antibodies are currently available for the treatment of autoimmune diseases, such as psoriasis (127). Moreover, IL-17 inhibition has also been effective in the treatment of some cases of ICI irAEs (128,129). Interestingly, in some preclinical studies, inhibition of IL-17 was able to improve the anti-tumour effects of ICI therapy (130,131), while in another study, inhibition of IL-25/IL-17RA simultaneously showed anti-tumour effects and alleviated irAEs in mice (132).

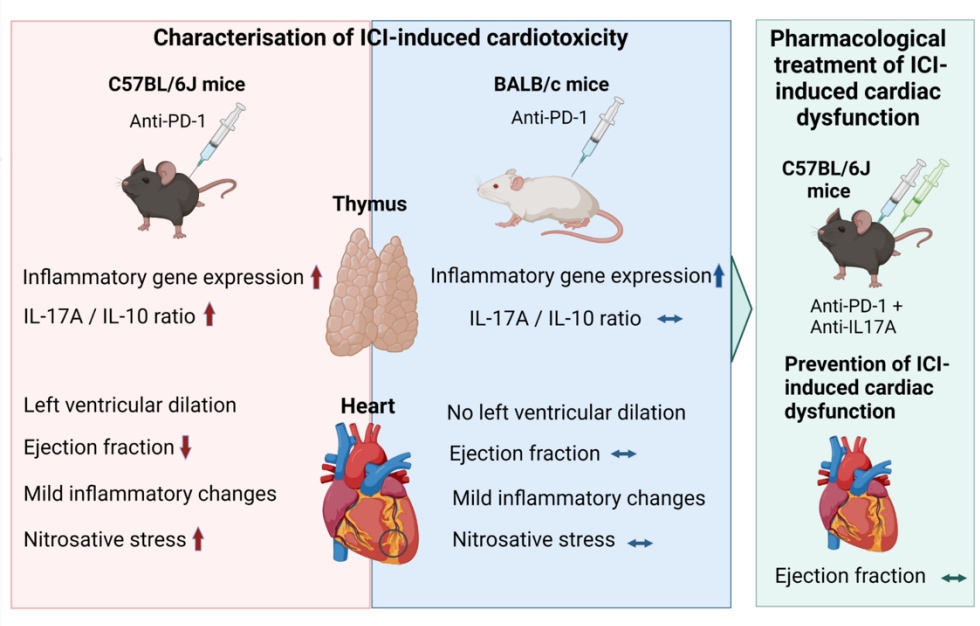

Figure 22. Summary of the first study. Immune checkpoint inhibitor (ICI)-induced cardiac dysfunction was alleviated with anti-IL17A treatment. PD-1: programmed cell death protein 1. Adapted from Gergely et al., Br. J. Pharmacol, 2023 *(89). Created via Biorender.com.*

In summary, anti-PD-1-induced cardiac dysfunction was shown to be mediated, at least in part, by systemic IL-17A signaling (Figure 22). Pharmacological inhibition of IL-17A may be a promising therapeutic strategy to alleviate ICI-induced cardiotoxicity while not interfering (or even improving) anti-cancer efficacy.

5.2 Hidden cardiotoxicity testing: use of bempedoic acid is safe in cardiac ischemia/reperfusion injury

Currently, hidden cardiotoxic effects of drugs, manifested only in pathological conditions of the heart, cannot be detected in the preclinical phases of drug development, as new investigational compounds are only tested on young, healthy animals, whereas models of cardiovascular diseases (e.g. ischemia/reperfusion injury, heart failure) or co-morbidities (e.g. diabetes, hypercholesterolemia) are not utilized (4). In a previous study, our group showed in a preclinical model of cardiac ischemia/reperfusion injury that rofecoxib induced lethal ventricular arrhythmias only in the presence of myocardial ischemia, thus exhibiting hidden cardiotoxic properties (76).

Investigating the hidden cardiotoxic properties of drugs that are indicated for the treatment of cardiovascular risk factors is of paramount importance, as the treated population is inherently more vulnerable to cardiac events. While antidiabetic drugs are required to undergo cardiovascular outcome trials before marketization (since the findings that rosiglitazone increased the risk of myocardial infarction, as discussed previously), antihyperlipidemic drugs may still be marketed based on the reduction of surrogate endpoints, such as LDL-cholesterol levels. In a preclinical study by *Kocsis et al.,* the antihyperlipidemic lovastatin was shown to interfere with the cardioprotective effects of ischemic conditioning, thus showing hidden cardiotoxic properties and suggesting that

during ischemic events, the myocardium may be more vulnerable to ischemia/reperfusion injury with the use of lovastatin (133).

Bempedoic acid is a novel, first-in-class lipid-lowering drug approved for the treatment of hypercholesterolemia and reduction of cardiovascular events. The long-term cardiovascular effects of bempedoic acid were investigated in the CLEAR Outcomes trial in patients with statin intolerance, where the primary analysis revealed a decreased occurrence of major adverse cardiac events with bempedoic acid use (134). However, in secondary analysis, the beneficial effects were found to be stronger in primary prevention indication (86), whereas in secondary prevention (in patients with established cardiovascular disease), even a possible harm, including a potential increase in all-cause and cardiovascular mortality, was seen (87). These findings raised the question of a potential hidden cardiotoxic effect in the diseased heart, which is not seen in patients with primary prevention.

Here, we investigated the effects of bempedoic acid during myocardial ischemia/reperfusion injury. We have found that long-term pretreatment with bempedoic acid did not exacerbate infarct size, arrhythmias, or mortality during ischemia/reperfusion, thus, it did not exhibit hidden cardiotoxic properties in this experimental setting. These findings suggest that bempedoic acid may be safe to use in patients at high risk for myocardial infarction, as no interaction was found between bempedoic acid treatment and myocardial ischemia/reperfusion injury.

Moreover, chronic treatment with bempedoic acid did not affect systolic or diastolic myocardial function or cardiac morphology, assessed via echocardiography. Recently, ACLY, one the main targets of bempedoic acid, has been shown to play differing roles in the failing myocardium: ACLY was found maintain normal NAD^+/NADH balance, whereas a downregulation was observed in patients with heart failure with preserved ejection fraction (135), while in another study, ACLY was necessary for the metabolic adaptation of the heart, maintaining cardiac function (136). These studies suggest that inhibition of ACLY in the heart may lead to adverse cardiac effects, however, whether bempedoic acid can effectively inhibit ACLY in the myocardium is not known currently, as its activating enzyme, ACSVL1, is not expressed in the heart (137). In another study, however, ACLY was found to promote

myofibroblast formation and cardiac fibrosis in a pressure overload-induced heart failure model, whereas pharmacological inhibition of ACLY prevented the pro-fibrotic effects (138). Based on these results, further investigation of bempedoic acid in models of post-myocardial infarction or non-ischemic heart failure may be warranted.

In healthy human volunteers, bempedoic acid did not affect cardiac repolarization and QT length, suggesting no pro-arrhythmic effects in the healthy heart (139). However, no previous data were available regarding the electrophysiological effects of bempedoic acid in the diseased heart. Importantly, ischemia/reperfusion injury may interact with the drug-induced electrophysiological effects and may cause arrhythmias that are not evident in healthy conditions (4,76). These effects may be caused by inhibition of the repolarization reserve (140), among other potential mechanisms. Here, we have found that pretreatment with bempedoic acid did not exacerbate ischemia/reperfusion-induced arrhythmias. On the contrary, reperfusion-induced early non-sustained ventricular tachycardias were suppressed in the bempedoic acid-treated group, which effect needs further investigation to confirm a potential clinical relevance. Amelioration of ischemia/reperfusion-induced arrhythmias was also reported with other lipid-lowering drugs in preclinical studies, including statins (141–143) and PCSK9 inhibitors (144).

In contrast to hidden cardiotoxic effects, many lipid-lowering drugs have been shown to have pleiotropic, cardioprotective effects beyond decreasing cholesterol. For instance, in preclinical models, statins and PCSK9 inhibitors have been shown to decrease infarct size (133,144–149). For this reason, we included ischemic preconditioning (the gold standard preclinical method for cardioprotection) in our study design to be able to assess any potential cardioprotective effect of bempedoic acid as well. Here, we have found no improvement in infarct size with bempedoic acid pretreatment. This finding suggests that bempedoic acid may be inferior to statins and PCSK9 inhibitors in terms of beneficial pleiotropic effects. Nevertheless, some pleiotropic effects of bempedoic acid are also recognized, for example, the lowering of inflammation as assessed by decreased hsCRP levels (150–153), as well as a potential beneficial effect in improving metabolic-associated fatty liver disease (MAFLD) or steatohepatitis (154,155).

In summary, chronic bempedoic acid treatment did not show hidden cardiotoxic effects in a rat model of cardiac ischemia/reperfusion injury, suggesting its safe use during myocardial infarction. Nevertheless, based on clinical findings of a reduced beneficial effect in secondary prevention indication, further preclinical studies may be needed to investigate the effect of bempedoic acid in diseased hearts.

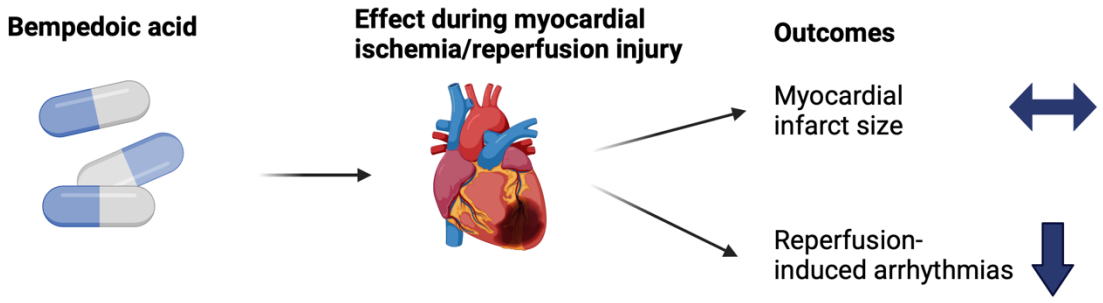

Figure 22. Summary of the second study. Bempedoic acid did not affect infarct size during acute myocardial ischemia/reperfusion injury, but it reduced reperfusion-induced arrhythmias. *Created via Biorender.com.*

5.3 Intersection of cardio-oncology and hidden cardiotoxicity: the need for risk stratification in cancer patients based on pre-existing cardiovascular diseases and risk factors

Whereas hidden cardiotoxicity is an emerging problem in drug development, cardiotoxic effects that are only seen or exacerbated in patients with diseased hearts may have further implications in cardio-oncology as well. Cancer patients with cardiovascular diseases or co-morbidities are often excluded from randomized clinical trials. For example, in the phase III Javelin Renal 101 trial (investigating avelumab, a PD-L1 inhibitor plus axitinib, compared with sunitinib treatment in renal cell carcinoma), using prospective cardiovascular surveillance, patients with a decreased LVEF, history of myocardial infarction or coronary revascularization, hypertension, or cerebrovascular events were excluded (156).

Nevertheless, patients with previous cardiovascular diseases may be at greater risk for the cardiovascular sequelae of anti-cancer medications. For example, pre-existing cardiovascular disease or cardiovascular risk factors are associated with cardiotoxicity after anthracycline

therapy (157–159), whereas coronary artery disease (160–163), diabetes (164), or obesity (161,165) were identified as risk factors for trastuzumab-induced cardiotoxicity.

In the case of immune checkpoint inhibitors, previously diagnosed ischemic heart disease or arrhythmias were found to predispose patients to major adverse cardiovascular events after ICI therapy in a retrospective observational study (166). In another study, a history of acute coronary syndrome or heart failure was associated with a higher incidence of myocarditis after ICI therapy (167). Moreover, in a preclinical model of hypertension-induced cardiac injury, increased myocardial inflammation was seen after anti-PD-1 treatment (168).

Overall, based on currently available data, risk assessment for cardiotoxic anti-cancer therapies should include pre-existing cardiovascular diseases or cardiometabolic risk factors. For example, the HFA-ICOS Cardio-Oncology cardiovascular risk assessment tool has been recently validated in anthracycline-induced cardiotoxicity, which involves information about previous cardiovascular diseases and risk factors of the patient (169). Nevertheless, the HFA-ICOS risk assessment only includes six anti-cancer medication groups (anthracyclines, HER-2 inhibitors, VEGF inhibitors, combined RAF/MEK inhibitors, multi-targeted kinase inhibitors, and multiple myeloma therapies), thus future research is needed to develop risk stratification systems for the remaining anti-cancer therapies with potential cardiovascular adverse effects, including immunotherapies.

6 CONCLUSIONS

In this PhD work, two fields of drug-induced cardiotoxicity were studied: (1) the mechanisms of the cardiotoxicity of a novel anti-cancer drug class, immune checkpoint inhibitors, and (2) the testing of hidden cardiotoxic effects of the novel antihyperlipidemic drug, bempedoic acid.

Here, we have shown that treatment with an anti-PD-1 immune checkpoint inhibitor monoclonal antibody induces cardiac dysfunction in C57BL/6J mice. This effect was associated with gene expression alterations in the myocardium and the thymus. Whereas only mild inflammatory changes were seen in the heart, prominent upregulation of pro-inflammatory markers was observed in the thymus, especially in the case of IL-17A. These findings suggested the involvement of systemic immune activation after anti-PD-1 treatment in cardiac dysfunction development. Further investigating this, BALB/c mice (a strain with Th2-type immune response as opposed to Th1 in C57BL/6J mice) were treated with anti-PD-1, where cardiac dysfunction was not evident, and the gene expression in the thymus was more balanced between the upregulation of pro-inflammatory and anti-inflammatory cytokines. Lastly, we co-treated C57BL/6J mice with anti-PD-1 and neutralizing anti-IL17A antibodies, which successfully prevented cardiac dysfunction development, suggesting the potential role of IL-17A blockade in ameliorating anti-PD-1-induced cardiac dysfunction.

Moreover, we have tested bempedoic acid, a novel antihyperlipidemic drug, in a preclinical model of cardiac ischemia/reperfusion injury for potential hidden cardiotoxic properties. Here, we have found that bempedoic acid did not elicit hidden cardiotoxic effects in rats, while it reduced reperfusion-induced arrhythmias. These findings suggest that bempedoic acid may be safely used during myocardial ischemia/reperfusion injury.

7 SUMMARY

The field of drug-induced cardiotoxicity investigates cardiovascular adverse effects of both oncological and non-oncological drugs. Cardiotoxicity of anti-cancer medications often results from the main mechanism of the drug and cannot be uncoupled from the anti-cancer effect. The use of novel anti-cancer therapies with potential cardiotoxic effects, such as immune checkpoint inhibitors, is increasing, thus, an understanding of the cardiotoxic mechanisms is needed to develop cardioprotective therapies. On the other hand, the cardiotoxicity of non-oncological drugs should be recognized early during drug development via mandatory screening studies. Nevertheless, some cardiotoxic effects of drugs may only manifest in the diseased hearts, which is currently not tested during preclinical drug development, a phenomenon termed “hidden cardiotoxicity”. Thus, cardiovascular adverse effects may only be seen after market authorization in some cases.

In our first study, we investigated the mechanisms of anti-PD-1-induced cardiotoxicity in multiple mouse models. Immune checkpoint inhibitors are known to cause cardiotoxic effects, however, the mechanisms are incompletely understood. Here, we found that anti-PD-1 treatment induced significant cardiac dysfunction in C57BL/6J, but not in BALB/c mice. A mild inflammatory response was seen in the myocardium of the animals, however, a markedly increased pro-inflammatory gene expression was observed in the thymus of C57BL/6J mice. Of note, *Il17a* showed the highest upregulation. Thus, we targeted IL-17A with a neutralizing antibody, which prevented the development of cardiac dysfunction after anti-PD-1 treatment. These findings suggest that IL-17A may be a promising therapeutic target to alleviate ICI-induced cardiotoxicity.

In our second study, we investigated the potential hidden cardiotoxic effects of bempedoic acid, a novel antihyperlipidemic drug. Here, we used a rat model of acute cardiac ischemia/reperfusion injury as a model for hidden cardiotoxicity testing. We found that chronic pretreatment with bempedoic acid did not show hidden cardiotoxic properties in this model, on the contrary, it reduced the occurrence of reperfusion-induced arrhythmias. These results suggest that the use of bempedoic acid may be safe during cardiac ischemia/reperfusion injury.

8 REFERENCES

1. Mamoshina P, Rodriguez B, Bueno-Orovio A. Toward a broader view of mechanisms of drug cardiotoxicity. Cell Rep Med . 2021;2(3):100216.
2. McNaughton R, Huet G, Shakir S. An investigation into drug products withdrawn from the EU market between 2002 and 2011 for safety reasons and the evidence used to support the decision-making. BMJ Open. 2014;4(1):1–7.
3. Onakpoya IJ, Heneghan CJ, Aronson JK. Post-marketing withdrawal of 462 medicinal products because of adverse drug reactions: A systematic review of the world literature. BMC Med . 2016;14(1):1–11.
4. Ferdinandy P, Baczko I, Bencsik P, Giricz Z, Gorbe A, Pacher P, et al. Definition of hidden drug cardiotoxicity: paradigm change in cardiac safety testing and its clinical implications. Eur Heart J . 2018;(July):1–10.
5. Ewer MS, Ewer SM. Cardiotoxicity of anticancer treatments: what the cardiologist needs to know. Nat Rev Cardiol . 2010;7(10):564–75.
6. Ewer MS, Ewer SM. Cardiotoxicity of anticancer treatments. Nat Rev Cardiol . 2015;12(9):547–58.
7. Herrmann J. Adverse cardiac effects of cancer therapies: cardiotoxicity and arrhythmia. Nat Rev Cardiol . 2020;1–29.
8. Herrmann J. Vascular toxic effects of cancer therapies. Nat Rev Cardiol . 2020;17(8):503–22.
9. Sawicki KT, Sala V, Prever L, Hirsch E, Ardehali H, Ghigo A. Preventing and Treating Anthracycline Cardiotoxicity: New Insights. Annu Rev Pharmacol Toxicol . 2021;61(Volume 61, 2021):309–32.
10. Amna Z, D. DZ, Ramya M, M. AR, Matthew L, Y. LU, et al. The Incidence, Risk Factors, and Outcomes With 5-Fluorouracil–Associated Coronary Vasospasm. JACC CardioOncol . 2021 Mar 1;3(1):101–9.
11. Nemeth BT, Varga Z V., Wu WJ, Pacher P. Trastuzumab cardiotoxicity: from clinical trials to experimental studies. Br J Pharmacol. 2017;174(21):3727–48.

12. Claire G, Sarah A, Kirsty M, Ashita W, Yi TY, C. PM, et al. Cardiotoxicity of BRAF/MEK Inhibitors. JACC CardioOncol . 2023 Oct 1;5(5):628–37.
13. Ball S, Ghosh RK, Wongsaengsak S, Bandyopadhyay D, Ghosh GC, Aronow WS, et al. Cardiovascular Toxicities of Immune Checkpoint Inhibitors: JACC Review Topic of the Week. J Am Coll Cardiol. 2019;74(13):1714–27.
14. Totzeck M, Michel L, Lin Y, Herrmann J, Rassaf T. Cardiotoxicity from chimeric antigen receptor-T cell therapy for advanced malignancies. Eur Heart J. 2022;43(20):1928–40.
15. Chen L, Flies DB. Molecular mechanisms of T cell co-stimulation and co-inhibition. Nat Rev Immunol . 2013;13(4):227–42.
16. He X, Xu C. Immune checkpoint signaling and cancer immunotherapy. Cell Res . 2020;30(8):660–9.
17. Rowshanravan B, Halliday N, Sansom DM. CTLA-4: a moving target in immunotherapy. Blood . 2018 Jan 4;131(1):58–67.
18. Oyewole-Said D, Konduri V, Vazquez-perez J, Weldon SA, Levitt JM, Decker WK. Beyond T-Cells : Functional Characterization of CTLA-4 Expression in Immune and Non-Immune Cell Types. Front Immunol. 2020;11(December).
19. Hossen MM, Ma Y, Yin Z, Xia Y, Du J, Huang JY, et al. Current understanding of CTLA-4: from mechanism to autoimmune diseases. Front Immunol . 2023;14.
20. Collins A V, Brodie DW, Gilbert RJC, Iaboni A, Manso-Sancho R, Walse B, et al. The Interaction Properties of Costimulatory Molecules Revisited. Immunity . 2002 Aug 1;17(2):201–10.
21. Schwartz JCD, Zhang X, Fedorov AA, Nathenson SG, Almo SC. Structural basis for co-stimulation by the human CTLA-4/B7-2 complex. Nature . 2001;410(6828):604–8.
22. Liu M, Yu Y, Hu S. A review on applications of abatacept in systemic rheumatic diseases. Int Immunopharmacol . 2021;96:107612.
23. Kitchens WH, Larsen CP, Badell IR. Costimulatory Blockade and Solid Organ Transplantation: The Past, Present, and Future. Kidney Int Rep . 2023;8(12):2529–45.

24. Buchbinder EI, Desai A. CTLA-4 and PD-1 Pathways: Similarities, Differences, and Implications of Their Inhibition. Am J Clin Oncol . 2016;39(1).
25. Fife BT, Pauken KE. The role of the PD-1 pathway in autoimmunity and peripheral tolerance. Ann N Y Acad Sci . 2011 Jan 1;1217(1):45–59.
26. Bracamonte-Baran W, Gilotra NA, Won T, Rodriguez KM, Talor M V., Oh BC, et al. Endothelial Stromal PD-L1 (Programmed Death Ligand 1) Modulates CD8+ T-Cell Infiltration After Heart Transplantation. Circ Heart Fail. 2021;14(10):e007982.
27. Cha JH, Chan LC, Li CW, Hsu JL, Hung MC. Mechanisms Controlling PD-L1 Expression in Cancer. Mol Cell . 2019;76(3):359–70.
28. Hodi FS, O'Day SJ, McDermott DF, Weber RW, Sosman JA, Haanen JB, et al. Improved Survival with Ipilimumab in Patients with Metastatic Melanoma. New England Journal of Medicine . 2010 Jun 10;363(8):711–23.
29. Robert C, Thomas L, Bondarenko I, O'Day S, Weber J, Garbe C, et al. Ipilimumab plus Dacarbazine for Previously Untreated Metastatic Melanoma. New England Journal of Medicine . 2011 Jun 5;364(26):2517–26.
30. Rizvi NA, Mazières J, Planchard D, Stinchcombe TE, Dy GK, Antonia SJ, et al. Activity and safety of nivolumab, an anti-PD-1 immune checkpoint inhibitor, for patients with advanced, refractory squamous non-small-cell lung cancer (CheckMate 063): A phase 2, single-arm trial. Lancet Oncol. 2015;16(3):257–65.
31. Balar A V., Castellano D, O'Donnell PH, Grivas P, Vuky J, Powles T, et al. First-line pembrolizumab in cisplatin-ineligible patients with locally advanced and unresectable or metastatic urothelial cancer (KEYNOTE-052): a multicentre, single-arm, phase 2 study. Lancet Oncol . 2017;18(11):1483–92.
32. Larkin J, Chiarion-Sileni V, Gonzalez R, Grob JJ, Cowey CL, Lao CD, et al. Combined Nivolumab and Ipilimumab or Monotherapy in Untreated Melanoma. New England Journal of Medicine . 2015 May 31;373(1):23–34.
33. Wolchok JD, Chiarion-Sileni V, Gonzalez R, Rutkowski P, Grob JJ, Cowey CL, et al. Overall Survival with Combined Nivolumab and Ipilimumab in Advanced Melanoma. New England Journal of Medicine . 2017 Sep 11;377(14):1345–56.

34. Upadhaya S, Neftelinov ST, Hodge J, Campbell J. Challenges and opportunities in the PD1/PDL1 inhibitor clinical trial landscape. Nat Rev Drug Discov. 2022;21(7):482–3.
35. Gergely TG, Drobni ZD, Sayour N V, Ferdinandy P, Varga Z V. Molecular fingerprints of cardiovascular toxicities of immune checkpoint inhibitors. Basic Res Cardiol . 2024;(0123456789).
36. Postow MA, Sidlow R, Hellmann MD. Immune-related adverse events associated with immune checkpoint blockade. New England Journal of Medicine. 2018;378(2):158–68.
37. Dougan M, Wang Y, Rubio-Tapia A, Lim JK. AGA Clinical Practice Update on Diagnosis and Management of Immune Checkpoint Inhibitor Colitis and Hepatitis: Expert Review. Gastroenterology . 2021 Mar 1;160(4):1384–93.
38. Kawsar A, Hussain K, Muinonen-Martin AJ, Fearfield L. How to recognize and manage skin toxicities associated with immune checkpoint inhibitors: a practical approach. British Journal of Dermatology . 2023 Oct 15;189(Supplement_1):i3–10.
39. Cunningham M, Gupta R, Butler M. Checkpoint inhibitor hepatotoxicity: pathogenesis and management. Hepatology . 2024;79(1).
40. Karaviti D, Kani ER, Karaviti E, Gerontiti E, Michalopoulou O, Stefanaki K, et al. Thyroid disorders induced by immune checkpoint inhibitors. Endocrine . 2024;85(1):67–79.
41. Farooq MZ, Aqeel SB, Lingamaneni P, Pichardo RC, Jawed A, Khalid S, et al. Association of Immune Checkpoint Inhibitors With Neurologic Adverse Events: A Systematic Review and Meta-analysis. JAMA Netw Open . 2022 Apr 19;5(4):e227722–e227722.
42. Miao J, Sise ME, Herrmann SM. Immune checkpoint inhibitor related nephrotoxicity: Advances in clinicopathologic features, noninvasive approaches, and therapeutic strategy and rechallenge. Frontiers in Nephrology . 2022;2.
43. Jo W, Won T, Daoud A, Čiháková D. Immune checkpoint inhibitors associated cardiovascular immune-related adverse events. Front Immunol. 2024;15(February):1–19.

44. Isawa T, Toi Y, Sugawara S, Taguri M, Toyoda S. Incidence, Clinical Characteristics, and Predictors of Cardiovascular Immune-Related Adverse Events Associated with Immune Checkpoint Inhibitors. Oncologist. 2022;27(5):e410–9.
45. Andres MS, Ramalingam S, Rosen SD, Baksi J, Khattar R, Kirichenko Y, et al. The spectrum of cardiovascular complications related to immune-checkpoint inhibitor treatment: Including myocarditis and the new entity of non inflammatory left ventricular dysfunction. Cardio-Oncology . 2022;8(1):1–11.
46. Lyon AR, Yousaf N, Battisti NML, Moslehi J, Larkin J. Immune checkpoint inhibitors and cardiovascular toxicity. Lancet Oncol. 2018;19(9):e447–58.
47. D'Souza M, Nielsen D, Svane IM, Iversen K, Rasmussen PV, Madelaire C, et al. The risk of cardiac events in patients receiving immune checkpoint inhibitors: a nationwide Danish study. Eur Heart J. 2020;1–11.
48. Salem JE, Manouchehri A, Moey M, Lebrun-Vignes B, Bastarache L, Pariente A, et al. Cardiovascular toxicities associated with immune checkpoint inhibitors: an observational, retrospective, pharmacovigilance study. Lancet Oncol . 2018;19(12):1579–89.
49. Drobni ZD, Alvi RM, Taron J, Zafar A, Murphy SP, Rambarat PK, et al. Association between Immune Checkpoint Inhibitors with Cardiovascular Events and Atherosclerotic Plaque. Circulation. 2020;2299–311.
50. Power JR, Alexandre J, Choudhary A, Ozbay B, Hayek S, Asnani A, et al. Electrocardiographic Manifestations of Immune Checkpoint Inhibitor Myocarditis. Circulation . 2021 Nov 2;144(18):1521–3.
51. Michel L, Helfrich I, Hendgen-Cotta UB, Mincu RI, Korste S, Mrotzek SM, et al. Targeting early stages of cardiotoxicity from anti-PD1 immune checkpoint inhibitor therapy. Eur Heart J. 2022;43(4):316–29.
52. Dolladille C, Ederhy S, Allouche S, Dupas Q, Gervais R, Madelaine J, et al. Late cardiac adverse events in patients with cancer treated with immune checkpoint inhibitors. J Immunother Cancer. 2020;8(1):1–10.

53. Gergely TG, Drobni ZD, Kallikourdis M, Zhu H, Meijers WC, Neilan TG, et al. Immune checkpoints in cardiac physiology and pathology: therapeutic targets for heart failure. Nat Rev Cardiol . 2024;
54. Johnson DB, Balko JM, Compton ML, Chalkias S, Gorham J, Xu Y, et al. Fulminant Myocarditis with Combination Immune Checkpoint Blockade. New England Journal of Medicine. 2016;375(18):1749–55.
55. Läubli H, Balmelli C, Bossard M, Pfister O, Glatz K, Zippelius A. Acute heart failure due to autoimmune myocarditis under pembrolizumab treatment for metastatic melanoma. J Immunother Cancer . 2015;3(1):4–9.
56. Champion SN, Stone JR. Immune checkpoint inhibitor associated myocarditis occurs in both high-grade and low-grade forms. Modern Pathology . 2020;33(1):99–108.
57. Axelrod ML, Meijers WC, Screever EM, Qin J, Carroll MG, Sun X, et al. T cells specific for α-myosin drive immunotherapy-related myocarditis. Nature . 2022;611(November).
58. Won T, Kalinoski HM, Wood MK, Hughes DM, Jaime CM, Delgado P, et al. Cardiac myosin-specific autoimmune T cells contribute to immune-checkpoint-inhibitor-associated myocarditis. Cell Rep. 2022;41(6).
59. Fenioux C, Abbar B, Boussouar S, Bretagne M, Power JR, Moslehi JJ, et al. Thymus alterations and susceptibility to immune checkpoint inhibitor myocarditis. Nat Med. 2023;29(12):3100–10.
60. Lyon AR, López-Fernández T, Couch LS, Asteggiano R, Aznar MC, Bergler-Klein J, et al. 2022 ESC Guidelines on cardio-oncology developed in collaboration with the European Hematology Association (EHA), the European Society for Therapeutic Radiology and Oncology (ESTRO) and the International Cardio-Oncology Society (IC-OS): Developed by the t. Eur Heart J . 2022 Nov 1;43(41):4229–361.
61. Spencer C Wei, Wouter C Meijers, Margaret L Axelrod, Nana-Ama A.S. Anang, Elles M Screever, Elizabeth C Wescott, Douglas B. Johnson, Elizabeth Whitley, Lorenz Lehmann, Pierre-Yves Courand, James J Mancuso, Lauren E Himmel, Benedicte Lebrun-Vignes, Matthew JJM and JPA. A genetic mouse model recapitulates immune

checkpoint inhibitor-associated myocarditis and supports a mechanism-based therapeutic intervention. Cancer Discov. 2020;

62. Salem JE, Allenbach Y, Vozy A, Brechot N, Johnson DB, Moslehi JJ, et al. Abatacept for Severe Immune Checkpoint Inhibitor–Associated Myocarditis. New England Journal of Medicine . 2019 Jun 12;380(24):2377–9.
63. Salem JE, Bretagne M, Abbar B, Leonard-Louis S, Ederhy S, Redheuil A, et al. Abatacept/Ruxolitinib and Screening for Concomitant Respiratory Muscle Failure to Mitigate Fatality of Immune-Checkpoint Inhibitor Myocarditis. Cancer Discov . 2023 May 4;13(5):1100–15.
64. Reynolds K, Mooradian M, Zlotoff D, Ridker P, Neilan T, Investigators TA. 696 Abatacept for immune checkpoint inhibitor associated myocarditis (ATRIUM): a phase 3, investigator-initiated, randomized, double blind, placebo-controlled trial. J Immunother Cancer . 2022 Nov 1;10(Suppl 2):A727 LP-A727.
65. Tisdale JE, Chung MK, Campbell KB, Hammadah M, Joglar JA, Leclerc J, et al. Drug-Induced Arrhythmias: A Scientific Statement From the American Heart Association. Circulation . 2020 Oct 13;142(15):e214–33.
66. Mamoshina P, Rodriguez B, Bueno-Orovio A. Toward a broader view of mechanisms of drug cardiotoxicity. Cell Rep Med . 2021;2(3):100216.
67. Nissen SE, Wolski K. Effect of Rosiglitazone on the Risk of Myocardial Infarction and Death from Cardiovascular Causes. New England Journal of Medicine. 2007;
68. Page RL, O'Bryant CL, Cheng D, Dow TJ, Ky B, Stein CM, et al. Drugs That May Cause or Exacerbate Heart Failure. Circulation . 2016 Aug 9;134(6):e32–69.
69. Bhattacharyya S, Schapira AH, Mikhailidis DP, Davar J. Drug-induced fibrotic valvular heart disease. The Lancet . 2009 Aug 15;374(9689):577–85.
70. ICH. https://www.ich.org/fileadmin/Public_Web_Site/ICH_Products/Guidelines/Safety/S7A/Step4/S7A_Guideline.pdf. 2000. Safety pharmacology studies for human pharmaceuticals S7A.
71. ICH. https://www.ich.org/fileadmin/Public_Web_Site/ICH_Products/Guidelines/Safety/S

7B/Step4/S7B_Guideline.pdf. 2005. The non-clinical evaluation of the potential for delayed ventricular repolarization (QT interval prolongation) by human pharmaceuticals S7B.

72. Ferraz MB, Bombardier C, Day R, Hawkey CJ, Laine L, Shapiro D, et al. Comparison of upper gastrointestinal toxicity of rofecoxib and naproxen in patients with rheumatoid arthritis. VIGOR Study Group. N Engl J Med . 2000;343(21):1520–8, 2 p following 1528.
73. Bresalier RS, Sandler RS, Quan H, Bolognese J a, Oxenius B, Horgan K, et al. Cardiovascular events associated with rofecoxib in a colorectal adenoma chemoprevention trial. Adenomatous Polyp Prevention on Vioxx (APPROVe) Trial Investigators. The New England Journal of Medicine . 2005;352(11):1092–102.
74. Janet W, M. SJ, Margaret H. Regulatory Action on Rosiglitazone by the U.S. Food and Drug Administration. New England Journal of Medicine . 2024 Aug 18;363(16):1489–91.
75. Hirshberg B, Raz I. Impact of the U.S. Food and Drug Administration Cardiovascular Assessment Requirements on the Development of Novel Antidiabetes Drugs. Diabetes Care . 2011 Apr 22;34(Supplement_2):S101–6.
76. Brenner GB, Makkos A, Nagy CT, Onódi Z, Sayour N V., Gergely TG, et al. Hidden Cardiotoxicity of Rofecoxib Can be Revealed in Experimental Models of Ischemia/Reperfusion. Cells. 2020;9(3):551.
77. Weber BY, Brenner GB, Kiss B, Gergely TG, Sayour N V., Tian H, et al. Rosiglitazone Does Not Show Major Hidden Cardiotoxicity in Models of Ischemia/Reperfusion but Abolishes Ischemic Preconditioning-Induced Antiarrhythmic Effects in Rats In Vivo. Pharmaceuticals. 2022;15(9).
78. Saeed A, Ballantyne CM. Bempedoic Acid (ETC-1002): A Current Review. Cardiol Clin . 2018;36(2):257–64.
79. Pinkosky SL, Newton RS, Day EA, Ford RJ, Lhotak S, Austin RC, et al. Liver-specific ATP-citrate lyase inhibition by bempedoic acid decreases LDL-C and attenuates atherosclerosis. Nat Commun. 2016;7(May).

80. Bytyçi I, Penson PE, Mikhailidis DP, Wong ND, Hernandez A V, Sahebkar A, et al. Prevalence of statin intolerance: a meta-analysis . Eur Heart J . 2022 Sep 7;43(34):3213–23.
81. Warden BA, Guyton JR, Kovacs AC, Durham JA, Jones LK, Dixon DL, et al. Assessment and management of statin-associated muscle symptoms (SAMS): A clinical perspective from the National Lipid Association. J Clin Lipidol . 2023;17(1):19–39.
82. Pinkosky SL, Filippov S, Srivastava RAK, Hanselman JC, Bradshaw CD, Hurley TR, et al. AMP-activated protein kinase and ATP-citrate lyase are two distinct molecular targets for ETC-1002, a novel small molecule regulator of lipid and carbohydrate metabolism. J Lipid Res. 2013;54(1):134–51.
83. Samsoondar JP, Burke AC, Sutherland BG, Telford DE, Sawyez CG, Edwards JY, et al. Prevention of diet-induced metabolic dysregulation, inflammation, and atherosclerosis in Ldlr-/- mice by treatment with the ATP-citrate lyase inhibitor bempedoic acid. Arterioscler Thromb Vasc Biol. 2017;37(4):647–56.
84. Ruscica M, Banach M, Sahebkar A, Corsini A, Sirtori CR. ETC-1002 (Bempedoic acid) for the management of hyperlipidemia: from preclinical studies to phase 3 trials. Expert Opin Pharmacother . 2019;20(7):791–803.
85. E. NS, Michael LA, Danielle B, K. RK, Denise M, J.P. KJ, et al. Bempedoic Acid and Cardiovascular Outcomes in Statin-Intolerant Patients. New England Journal of Medicine . 2023 Apr 12;388(15):1353–64.
86. Nissen SE, Menon V, Nicholls SJ, Brennan D, Laffin L, Ridker P, et al. Bempedoic Acid for Primary Prevention of Cardiovascular Events in Statin-Intolerant Patients. JAMA . 2023 Jul 11;330(2):131–40.
87. Sayed A, Brophy JM. Effect of bempedoic acid on mortality and cardiovascular events in primary and secondary prevention: A post-hoc analysis of the CLEAR-outcomes trial. Int J Cardiol . 2024;406(April):132074.
88. Gergely TG, Brenner GB, Nagy RN, Sayour N V, Makkos A, Kovácsházi C, et al. Effects of Bempedoic Acid in Acute Myocardial Infarction in Rats: No Cardioprotection and No Hidden Cardiotoxicity. Int J Mol Sci. 2023;24(2).

89. Gergely TG, Kucsera D, Tóth VE, Kovács T, Sayour N V., Drobni ZD, et al. Characterization of immune checkpoint inhibitor-induced cardiotoxicity reveals interleukin-17A as a driver of cardiac dysfunction after anti-PD-1 treatment. Br J Pharmacol. 2022;(February):1–22.
90. du Sert NP, Hurst V, Ahluwalia A, Alam S, Avey MT, Baker M, et al. The arrive guidelines 2.0: Updated guidelines for reporting animal research. PLoS Biol. 2020;18(7):1–12.
91. Zacchigna S, Paldino A, Falcão-Pires I, Daskalopoulos EP, Dal Ferro M, Vodret S, et al. Towards standardization of echocardiography for the evaluation of left ventricular function in adult rodents: A position paper of the ESC Working Group on Myocardial Function. Cardiovasc Res. 2021;117(1):43–59.
92. Gergely TG, Kovács T, Kovács A, Tóth VE, Sayour N V., Mórotz GM, et al. CardiLect: A combined cross-species lectin histochemistry protocol for the automated analysis of cardiac remodelling. ESC Heart Fail. 2024 Apr 1;
93. Martin M. Cutadapt removes adapter sequences from high-throughput sequencing reads. EMBnet J. 2011;17:10–2.
94. Ewels P, Magnusson M, Lundin S, Käller M. MultiQC: Summarize analysis results for multiple tools and samples in a single report. Bioinformatics. 2016;32(19):3047–8.
95. Yates A, Akanni W, Amode MR, Barrell D, Billis K, Carvalho-Silva D, et al. Ensembl 2016. Nucleic Acids Res. 2016;44(D1):D710–6.
96. Kim D, Paggi JM, Park C, Bennett C, Salzberg SL. Graph-based genome alignment and genotyping with HISAT2 and HISAT-genotype. Nat Biotechnol . 2019;37(8):907–15.
97. Liao Y, Smyth GK, Shi W. FeatureCounts: An efficient general purpose program for assigning sequence reads to genomic features. Bioinformatics. 2014;30(7):923–30.
98. Love MI, Huber W, Anders S. Moderated estimation of fold change and dispersion for RNA-seq data with DESeq2. Genome Biol. 2014;15(12):1–21.

99. Benjamini Y, Hochberg Y. Controlling the False Discovery Rate: A Practical and Powerful Approach to Multiple Testing. Journal of the Royal Statistical Society Series B (Methodological) . 1995;57(1):289–300.
100. Mi H, Muruganujan A, Ebert D, Huang X, Thomas PD. PANTHER version 14: More genomes, a new PANTHER GO-slim and improvements in enrichment analysis tools. Nucleic Acids Res. 2019;47(D1):D419–26.
101. Curtis MJ, Walker MJA. Quantification of arrhythmias using scoring systems: An examination of seven scores in an in vivo model of regional myocardial ischaemia. Cardiovascular Research. 1988.
102. Curtis MJ, Hancox JC, Farkas A, Wainwright CL, Stables CL, Saint DA, et al. The lambeth conventions (II): Guidelines for the study of animal and human ventricular and supraventricular arrhythmias. Pharmacology and Therapeutics. 2013.
103. Watanabe H, Numata K, Ito T, Takagi K, Matsukawa A. Innate immune response in Th1- and Th2-dominant mouse strains. 2004;22(5):460–6.
104. Haslam A, Gill J, Prasad V. Estimation of the Percentage of US Patients With Cancer Who Are Eligible for Immune Checkpoint Inhibitor Drugs. JAMA Netw Open . 2020 Mar 9;3(3):e200423–e200423.
105. Dolladille C, Akroun J, Morice PM, Dompmartin A, Ezine E, Sassier M, et al. Cardiovascular immunotoxicities associated with immune checkpoint inhibitors: A safety meta-analysis. Eur Heart J. 2021;42(48):4964–77.
106. Laenens D, Yu Y, Santens B, Jacobs J, Beuselinck B, Bechter O, et al. Incidence of Cardiovascular Events in Patients Treated with Immune Checkpoint Inhibitors. Journal of Clinical Oncology. 2022;40(29):3430–8.
107. Tay WT, Fang YH, Beh ST, Liu YW, Hsu LW, Yen CJ, et al. Programmed cell death-1: Programmed cell death-ligand 1 interaction protects human cardiomyocytes against T-cell mediated inflammation and apoptosis response in vitro. Int J Mol Sci. 2020;21(7).
108. Nishimura H, Okazaki T, Tanaka Y, Nakatani K, Hara M, Matsumori A, et al. Autoimmune dilated cardiomyopathy in PD-1 receptor-deficient mice. Science (1979). 2001;291(5502):319–22.

109. Okazaki T, Tanaka Y, Nishio R, Mitsuiye T, Mizoguchi A, Wang J, et al. Autoantibodies against cardiac troponin I are responsible for dilated cardiomyopathy in PD-1-deficient mice. Nat Med. 2003;9(12):1477–83.
110. Weber J, Mandala M, Del Vecchio M, Gogas HJ, Arance AM, Cowey CL, et al. Adjuvant Nivolumab versus Ipilimumab in Resected Stage III or IV Melanoma. New England Journal of Medicine. 2017;377(19):1824–35.
111. Huang YV, Lee D, Sun Y, Chou H, Xu B, Lin Z, et al. A Novel Therapeutic Approach using CXCR3 Blockade to Treat Immune Checkpoint Inhibitor-mediated Myocarditis. bioRxiv . 2024 Jan 1;2024.01.30.576279.
112. Ma P, Liu J, Qin J, Lai L, Heo GS, Luehmann H, et al. Expansion of Pathogenic Cardiac Macrophages in Immune Checkpoint Inhibitor Myocarditis. Circulation . 2024 Jan 2;149(1):48–66.
113. Ngwenyama N, Salvador AM, Velázquez F, Nevers T, Levy A, Aronovitz M, et al. CXCR3 regulates CD4+ T cell cardiotropism in pressure overload–induced cardiac dysfunction. JCI Insight. 2019;4(7).
114. Khan S, Khan SA, Luo X, Fattah FJ, Saltarski J, Gloria-McCutchen Y, et al. Immune dysregulation in cancer patients developing immune-related adverse events. Br J Cancer . 2019;120(1):63–8.
115. Altara R, Mallat Z, Booz GW, Zouein FA. The CXCL10/CXCR3 Axis and Cardiac Inflammation: Implications for Immunotherapy to Treat Infectious and Noninfectious Diseases of the Heart. J Immunol Res. 2016;2016.
116. Konstantina T, Konstantinos R, Anastasios K, Anastasia M, Eleni L, Ioannis S, et al. Fatal adverse events in two thymoma patients treated with anti-PD-1 immune check point inhibitor and literature review. Lung Cancer. 2019;135(April):29–32.
117. Mencel J, Gargett T, Karanth N, Pokorny A, Brown MP, Charakidis M. Thymic hyperplasia following double immune checkpoint inhibitor therapy in two patients with stage IV melanoma. Asia Pac J Clin Oncol. 2019;15(6):383–6.
118. Dulos J, Carven GJ, Van Boxtel SJ, Evers S, Driessen-Engels LJA, Hobo W, et al. PD-1 blockade augments Th1 and Th17 and suppresses Th2 responses in peripheral

blood from patients with prostate and advanced melanoma cancer. Journal of Immunotherapy. 2012;35(2):169–78.

119. Tarhini AA, Zahoor H, Lin Y, Malhotra U, Sander C, Butterfield LH, et al. Baseline circulating IL-17 predicts toxicity while TGF-β1 and IL-10 are prognostic of relapse in ipilimumab neoadjuvant therapy of melanoma. J Immunother Cancer . 2015;3(1):15–20.
120. von Euw E, Chodon T, Attar N, Jalil J, Koya RC, Comin-Anduix B, et al. CTLA4 blockade increases Th17 cells in patients with metastatic melanoma. J Transl Med. 2009;7:1–13.
121. Baldeviano GC, Barin JG, Talor M V., Srinivasan S, Bedja D, Zheng D, et al. Interleukin-17A is dispensable for myocarditis but essential for the progression to dilated cardiomyopathy. Circ Res. 2010;106(10):1646–55.
122. Shang AQ, Yu CJ, Bi X, Jiang WW, Zhao ML, Sun Y, et al. Blocking CTLA-4 promotes pressure overload-induced heart failure via activating Th17 cells. The FASEB Journal . 2024 Aug 15;38(15):e23851.
123. Myers JM, Cooper LT, Kem DC, Stavrakis S, Kosanke SD, Shevach EM, et al. Cardiac myosin-Th17 responses promote heart failure in human myocarditis. JCI Insight. 2016;1(9).
124. Baumhove L, van Essen BJ, Dokter MM, Zijlstra SN, Deiman FE, Laman JD, et al. IL-17 is associated with disease severity and targetable inflammatory processes in heart failure. ESC Heart Fail . 2024 Jul 19.
125. Xue G long, Li D sheng, Wang Z yong, Liu Y, Yang J ming, Li C zhu, et al. Interleukin-17 upregulation participates in the pathogenesis of heart failure in mice via NF- κ B-dependent suppression of SERCA2a and Cav1 . 2 expression. Acta Pharmacol Sin. 2021;42(February):1780–9.
126. Yagi J, Arimura Y, Takatori H, Nakajima H, Iwamoto I, Uchiyama T. Genetic background influences Th cell differentiation by controlling the capacity for IL-2-induced IL-4 production by naive CD4+ T cells. Int Immunol . 2006 Dec 1;18(12):1681–90.

127. Ghoreschi K, Balato A, Enerbäck C, Sabat R. Therapeutics Therapeutics targeting the IL-23 and IL-17 pathway in psoriasis. Lancet. 2021;397(754):766.
128. Johnson D, Patel AB, Uemura MI, Trinh VA, Jackson N, Zobniw CM, et al. IL17A Blockade Successfully Treated Psoriasiform Dermatologic Toxicity from Immunotherapy. Cancer Immunol Res. 2019;7(June):860–5.
129. Lechner MG, Cheng MI, Patel AY, Hoang T, Yakobian N, Astourian M, et al. Inhibition of IL-17A Protects against Thyroid Immune-Related Adverse Events while Preserving Checkpoint Inhibitor Antitumor Efficacy. The Journal of Immunology. 2022;209:1–14.
130. Liu C, Liu R, Wang B, Lian J, Yao Y, Sun H, et al. Blocking IL-17A enhances tumor response to anti-PD-1 immunotherapy in microsatellite stable colorectal cancer. J Immunother Cancer. 2021;9(1).
131. Nagaoka K, Shirai M, Taniguchi K, Hosoi A, Sun C, Kobayashi Y, et al. Deep immunophenotyping at the cell level identifies a combination of anti- IL-17 and checkpoint blockade as an effective treatment in a preclinical model of data- guided personalized immunotherapy. J Immunother Cancer. 2020;1–14.
132. Hu X, Bukhari SM, Tymm C, Adam K, Lerrer S, Henick BS, et al. Inhibition of IL-25/IL-17RA improves immune-related adverse events of checkpoint inhibitors and reveals antitumor activity. J Immunother Cancer . 2024 Mar 1;12(3):e008482.
133. Kocsis GF, Pipis J, Fekete V, Kovács-Simon A, Odendaal L, Molnár É, et al. Lovastatin interferes with the infarct size-limiting effect of ischemic preconditioning and postconditioning in rat hearts. Am J Physiol Heart Circ Physiol. 2008;294(5):2406–9.
134. Nissen SE, Lincoff AM, Brennan D, Ray KK, Mason D, Kastelein JJP, et al. Bempedoic Acid and Cardiovascular Outcomes in Statin-Intolerant Patients. New England Journal of Medicine. 2023;388(15):1353–64.
135. Meddeb M, Koleini N, Jun S, Keykhaei M, Farshidfar F, Zhao L, et al. ATP Citrate Lyase Supports Cardiac Function and NAD+/NADH Balance And Is Depressed in Human Heart Failure. bioRxiv . 2024 Jan 1;2024.06.09.598152.

136. Liu S, Gammon ST, Tan L, Gao Y, Kim K, Williamson IK, et al. ATP-dependent citrate lyase Drives Left Ventricular Dysfunction by Metabolic Remodeling of the Heart. bioRxiv . 2024 Jan 1;2024.06.21.600099.
137. Watkins PA. Very-long-chain acyl-CoA synthetases. Journal of Biological Chemistry . 2008;283(4):1773–7.
138. Lazaropoulos MP, Gibb AA, Chapski DJ, Nair AA, Reiter AN, Roy R, et al. Nuclear ATP-citrate lyase regulates chromatin-dependent activation and maintenance of the myofibroblast gene program. Nature Cardiovascular Research . 2024;3(7):869–82.
139. Amore BM, Cramer CT, Emery MG, Macdougall DE. Absence of effect of steady state bempedoic acid on cardiac repolarization : Results of a thorough QT / QTc study in healthy volunteers. 2021;(March):2487–96.
140. Varró A, Baczkó I. Cardiac ventricular repolarization reserve: A principle for understanding drug-related proarrhythmic risk. British Journal of Pharmacology. 2011.
141. Andelova K, Bacova BS, Sykora M, Hlivak P, Barancik M, Tribulova N. Mechanisms Underlying Antiarrhythmic Properties of Cardioprotective Agents Impacting Inflammation and Oxidative Stress. Int J Mol Sci. 2022;23(3).
142. Chen J, Nagasawa Y, Zhu BM, Ohmori M, Harada KI, Fujimura A, et al. Pravastatin prevents arrhythmias induced by coronary artery ischemia/reperfusion in anesthetized normocholesterolemic rats. J Pharmacol Sci. 2003;93(1):87–94.
143. Thuc LC, Teshima Y, Takahashi N, Nishio S, Fukui A, Kume O, et al. Cardioprotective effects of pravastatin against lethal ventricular arrhythmias induced by reperfusion in the rat heart. Circulation Journal. 2011;75(7):1601–8.
144. Palee S, McSweeney CM, Maneechote C, Moisescu DM, Jaiwongkam T, Kerdphoo S, et al. PCSK9 inhibitor improves cardiac function and reduces infarct size in rats with ischaemia/reperfusion injury: Benefits beyond lipid-lowering effects. J Cell Mol Med. 2019;23(11):7310–9.
145. Mendieta G, Ben-Aicha S, Gutiérrez M, Casani L, Aržanauskaitė M, Carreras F, et al. Intravenous Statin Administration During Myocardial Infarction Compared With Oral Post-Infarct Administration. J Am Coll Cardiol. 2020;75(12):1386–402.

146. Andreadou I, Farmakis D, Prokovas E, Sigala F, Zoga A, Spyridaki K, et al. Short-term statin administration in hypercholesterolaemic rabbits resistant to postconditioning: Effects on infarct size, endothelial nitric oxide synthase, and nitro-oxidative stress. Cardiovasc Res. 2012;94(3):501–9.
147. Wolfrum S, Dendorfer A, Schutt M, Weidtmann B, Heep A, Tempel K, et al. Simvastatin acutely reduces myocardial reperfusion injury in vivo by activating the phosphatidylinositide 3-kinase/Akt pathway. J Cardiovasc Pharmacol. 2004;44(3):348–55.
148. Ding Z, Wang X, Liu S, Shahanawaz J, Theus S, Fan Y, et al. PCSK9 expression in the ischaemic heart and its relationship to infarct size, cardiac function, and development of autophagy. Cardiovasc Res. 2018;114(13):1738–51.
149. Schreckenberg R, Wolf A, Szabados T, Gömöri K, Szabó IA, Ágoston G, et al. Proprotein Convertase Subtilisin Kexin Type 9 (PCSK9) Deletion but not Inhibition of Extracellular PCSK9 Reduces Infarct Sizes Ex Vivo but not In Vivo. Int J Mol Sci. 2022;23(12).
150. Cicero AFG, Fogacci F, Hernandez A V., Banach M, Alnouri F, Amar F, et al. Efficacy and safety of bempedoic acid for the treatment of hypercholesterolemia: A systematic review and meta-analysis. PLoS Med . 2020;17(7):1–21.
151. Ridker PM, Lei L, Ray KK, Ballantyne CM, Bradwin G, Rifai N. Effects of bempedoic acid on CRP, IL-6, fibrinogen and lipoprotein(a) in patients with residual inflammatory risk: A secondary analysis of the CLEAR harmony trial. J Clin Lipidol . 2023;17(2):297–302.
152. Ridker PM, Lei L, Louie MJ, Haddad T, Nicholls SJ, Lincoff AM, et al. Inflammation and Cholesterol as Predictors of Cardiovascular Events Among 13 970 Contemporary High-Risk Patients With Statin Intolerance. Circulation . 2024 Jan 2;149(1):28–35.
153. Stroes ESG, Bays HE, Banach M, Catapano AL, Duell PB, Laufs U, et al. Bempedoic acid lowers high-sensitivity C-reactive protein and low-density lipoprotein cholesterol: Analysis of pooled data from four phase 3 clinical trials. Atherosclerosis . 2023;373:1–9.

154. Morrow MR, Batchuluun B, Wu J, Ahmadi E, Leroux JM, Mohammadi-Shemirani P, et al. Inhibition of ATP-citrate lyase improves NASH, liver fibrosis, and dyslipidemia. Cell Metab . 2022;34(6):919-936.e8.
155. Anasdeen S M, S S, TM V. Evaluating Bempedoic Acid for Non-alcoholic Fatty Liver Disease: A Review of Preclinical and Clinical Research. Cureus . 2024;16(8):e67151.
156. Rini BI, Moslehi JJ, Bonaca M, Schmidinger M, Albiges L, Choueiri TK, et al. Prospective Cardiovascular Surveillance of Immune Checkpoint Inhibitor-Based Combination Therapy in Patients with Advanced Renal Cell Cancer: Data from the Phase III JAVELIN Renal 101 Trial. Journal of Clinical Oncology. 2022;40(17):1929–38.
157. Ryberg M, Nielsen D, Cortese G, Nielsen G, Skovsgaard T, Andersen PK. New Insight Into Epirubicin Cardiac Toxicity: Competing Risks Analysis of 1097 Breast Cancer Patients. JNCI: Journal of the National Cancer Institute . 2008 Aug 6;100(15):1058–67.
158. Qiu S, Zhou T, Qiu B, Zhang Y, Zhou Y, Yu H, et al. Risk Factors for Anthracycline-Induced Cardiotoxicity. Front Cardiovasc Med . 2021;8.
159. Cai F, Luis Antonio Falar M, Lin X, Wang M, Cai L, Cen C, et al. Anthracycline-induced cardiotoxicity in the chemotherapy treatment of breast cancer: Preventive strategies and treatment (Review). Mol Clin Oncol . 2019;11(1):15–23.
160. Tang GH, Acuna SA, Sevick L, Yan AT, Brezden-Masley C. Incidence and identification of risk factors for trastuzumab-induced cardiotoxicity in breast cancer patients: an audit of a single “real-world” setting. Medical Oncology . 2017;34(9):154.
161. Gunaldi M, Duman BB, Afsar CU, Paydas S, Erkisi M, Kara IO, et al. Risk factors for developing cardiotoxicity of trastuzumab in breast cancer patients: An observational single-centre study. Journal of Oncology Pharmacy Practice . 2015 Jan 7;22(2):242–7.
162. Chavez-MacGregor M, Zhang N, Buchholz TA, Zhang Y, Niu J, Elting L, et al. Trastuzumab-Related Cardiotoxicity Among Older Patients With Breast Cancer. Journal of Clinical Oncology . 2013 Oct 14;31(33):4222–8.

163. Ezaz G, Long JB, Gross CP, Chen J. Risk Prediction Model for Heart Failure and Cardiomyopathy After Adjuvant Trastuzumab Therapy for Breast Cancer. J Am Heart Assoc . 2024 Aug 20;3(1):e000472.
164. Serrano C, Cortés J, De Mattos-Arruda L, Bellet M, Gómez P, Saura C, et al. Trastuzumab-related cardiotoxicity in the elderly: a role for cardiovascular risk factors. Annals of Oncology . 2012 Apr 1;23(4):897–902.
165. Guenancia C, Lefebvre A, Cardinale D, Yu AF, Ladoire S, Ghiringhelli F, et al. Obesity As a Risk Factor for Anthracyclines and Trastuzumab Cardiotoxicity in Breast Cancer: A Systematic Review and Meta-Analysis. Journal of Clinical Oncology . 2016 Jul 25;34(26):3157–65.
166. Torrente M, Blanco M, Franco F, Garitaonaindia Y, Calvo V, Collazo-Lorduy A, et al. Assessing the risk of cardiovascular events in patients receiving immune checkpoint inhibitors. Front Cardiovasc Med. 2022;9(December):1–10.
167. Oren O, Yang EH, Molina JR, Bailey KR, Blumenthal RS, Kopecky SL. Cardiovascular Health and Outcomes in Cancer Patients Receiving Immune Checkpoint Inhibitors. American Journal of Cardiology . 2020 Jun 15;125(12):1920–6.
168. Rubio-Infante N, Castillo EC, Alves-Figueiredo H, Ramos-González M, Salazar-Ramírez F, Salas-Treviño D, et al. Previous cardiovascular injury is a prerequisite for immune checkpoint inhibitor-associated lethal myocarditis in mice. ESC Heart Fail . 2024 Apr 1;11(2):1249–57.
169. Rivero-Santana B, Saldaña-García J, Caro-Codón J, Zamora P, Moliner P, Martínez Monzonis A, et al. Anthracycline-induced cardiovascular toxicity: validation of the Heart Failure Association and International Cardio-Oncology Society risk score. Eur Heart J . 2024 Aug 6;ehae496.

9 LIST OF OWN PUBLICATIONS

9.1 Publications related to the Candidate's PhD dissertation

I. **Gergely, T. G.**, Kucsera, D., Tóth, V. E., Kovács, T., Sayour, N. V., Drobni, Z. D., Ruppert, M., Petrovich, B., Ágg, B., Onódi, Z., Fekete, N., Pállinger, É., Buzás, E. I., Yousif, L. I., Meijers, W. C., Radovits, T., Merkely, B., Ferdinandy, P., & Varga, Z. V. "Characterization of immune checkpoint inhibitor-induced cardiotoxicity reveals interleukin-17A as a driver of cardiac dysfunction after anti-PD-1 treatment." British Journal of Pharmacology, (2022) 1– 22.

IF: 6.8

II. **Gergely, T.G.***, Brenner, G.B.*, Nagy, R.N., Sayour, N.V., Makkos, A., Kovácsházi, C., Tian, H., Schulz, R., Giricz, Z., Görbe, A., Ferdinandy, P. "Effects of Bempedoic Acid in Acute Myocardial Infarction in Rats: No Cardioprotection and No Hidden Cardiotoxicity." Int. J. Mol. Sci. (2023), 24,1585.

IF: 4.9 *equal contribution to this study

∑IF of dissertation-related publications: 11.7

9.2 Publications independent of the Candidate's PhD dissertation

III. Bánfi-Bacsárdi F., Kazay Á.*, **Gergely T.G.**, Forrai Z., Füzesi T.P., Hanuska L.F., Schäffer P. P., Pilecky D., Vámos M., Vértes V., Dékány M, Andréka P., Piróth Z., Nyolczas N., Muk B "Therapeutic Consequences and Prognostic Impact of Mutlimorbidity in Heart Failure: Time to Act". J Clin Med. 2024 Dec 29;14(1):139.

IF: 3.0

IV. **Gergely T.G.**, Kovács T., Kovács A., Tóth V.E., Sayour N.V., Mórotz G.M., Kovácsházi C., Brenner G.B., Onódi Z., Enyedi B., Máthé D., Leszek P., Giricz Z., Ferdinandy P., Varga Z.V. "CardiLect: A combined cross-species lectin histochemistry protocol for the automated analysis of cardiac remodelling." ESC Heart Fail. 2024 Nov 13.

IF: 3.2

V. Sayour N.V., Kucsera D., Alhaddad A.R., Tóth V.É., **Gergely T.G.**, Kovács T., Hegedűs Z.I., Jakab M.E., Ferdinandy P., Varga Z.V. “Effects of sex and obesity on immune checkpoint inhibition-related cardiac systolic dysfunction in aged mice.” Basic Res Cardiol. 2024 Nov 8.

IF: 7.5

VI. Kestecher B.M., Németh K., Ghosal S., Sayour N.V., **Gergely T.G.**, Bodnár B.R., Försönits A.I., Sódar B.W., Oesterreicher J., Holnthoner W., Varga Z.V., Giricz Z., Ferdinandy P., Buzás E.I., Osteikoetxea X. “Reduced circulating $CD63^+$ extracellular vesicle levels associate with atherosclerosis in hypercholesterolaemic mice and humans.” Cardiovasc Diabetol. 2024 Oct 17;23(1):368.

IF: 8.5

VII. Bánfi-Bacsárdi F., Boldizsár E.M., **Gergely T.G.**, Forrai Z., Kazay Á., Füzesi T., Hanuska L.F., Schäffer P.P., Pilecky D., Vámos M., Gavallér Z., Keresztes K., Dékány M., Andréka P., Piróth Z., Nyolczas N., Muk B. [The role of complex patient education program in heart failure care]. Orv Hetil. 2024 Sep 15;165(37):1461-1471.

IF: 0.8

VIII. Sayour N.V., **Gergely T.G.**, Váradi B., Tóth V.É., Ágg B., Kovács T., Kucsera D., Kovácsházi C., Brenner G.B., Giricz Z., Ferdinandy P., Varga Z.V. “Comparison of mouse models of heart failure with reduced ejection fraction.” ESC Heart Fail. 2024 Sep 7

IF: 3.2

IX. **Gergely T.G.**, Bánfi-Bacsárdi F, Komáromi A, Pilecky D, Boldizsár EM, Flegler D, Kazay Á, Füzesi T, Forrai Z, Vértes V, Sayour VN, Andréka P, Piróth Z, Nyolczas N, Muk B. [Rapid up-titration of guide-directed medical therapy after a heart failure hospitalisation]. Orv Hetil. 2024 Aug 4;165(31):1197-1205.

IF: 0.8

X. **Gergely T.G.,** Drobni Z.D., Sayour N.V., Ferdinandy P., Varga Z.V. “Molecular fingerprints of cardiovascular toxicities of immune checkpoint inhibitors.” Basic Res Cardiol. 2024 Jul 17.

IF: 7.5

XI. Kovácsházi C., Hambalkó S., Sayour N.V., **Gergely T.G.**, Brenner G.B., Pelyhe C., Kapui D., Weber B.Y., Hültenschmidt A.L., Pállinger É., Buzás E.I., Zolcsák Á., Kiss B., Bozó T., Csányi C., Kósa N., Kellermayer M., Farkas R., Karvaly GB., Wynne K., Matallanas D., Ferdinandy P., Giricz Z.. "Effect of hypercholesterolemia on circulating and cardiomyocyte-derived extracellular vesicles." Sci Rep. 2024 May 26;14(1):12016

IF: 3.8

XII. Muk B., Pilecky D., Bánfi-Bacsárdi F., Füzesi T., **Gergely T.G.**, Komáromi A., Papp E., Szőnyi M.D., Forrai Z., Kazay Á., Solymossi B., Vámos M., Andréka P., Piróth Z., Nyolczas N. [The changes in the pharmacotherapy of heart failure with reduced ejection fraction and its effect on prognosis: experience in the Hungarian clinical practice]. Orv Hetil. 2024 May 5;165(18):698-710.

IF: 0.8

XIII. **Gergely T.G.,** Drobni Z.D., Kallikourdis M., Zhu H., Meijers W.C., Neilan T.G., Rassaf T., Ferdinandy P., Varga Z.V. "Immune checkpoints in cardiac physiology and pathology: therapeutic targets for heart failure." Nat Rev Cardiol (2024). Jul;21(7):443-462

IF: 41.7

XIV. Sayour N.V., Tóth V.É., Nagy R.N., Vörös I., **Gergely T.G.**, Onódi Z., Nagy N., Bödör C., Váradi B., Ruppert M., Radovits T., Bleckwedel F., Zelarayán L.C., Pacher P., Ágg B., Görbe A., Ferdinandy P., Varga Z.V., "Droplet Digital PCR Is a Novel Screening Method Identifying Potential Cardiac G-Protein-Coupled Receptors as Candidate Pharmacological Targets in a Rat Model of Pressure-Overload-Induced Cardiac Dysfunction." Int J Mol Sci. 2023 Sep 7;24(18):13826.

IF: 4.9

XV. Kucsera D., Tóth V.E., Sayour N.V., Kovács T., **Gergely T.G.**, Ruppert M., Radovits T., Fábián A., Kovács A., Merkely B., Ferdinandy P., Varga Z.V. "IL-1β neutralization prevents diastolic dysfunction development, but lacks hepatoprotective effect in an aged mouse model of NASH." Sci Rep 13, 356 (2023).

IF: 3.8

XVI. Sayour N.V., Brenner G.B., Makkos A., Kiss B., Kovácsházi C., **Gergely T.G.**, Aukrust S.G., Tian H., Zenkl V., Gömöri K., Szabados T., Bencsik P., Heinen A, Schulz R., Baxter G.F., Zuurbier C.J., Vokó Z., Ferdinandy P., Giricz Z. "Cardioprotective efficacy of limb remote ischemic preconditioning in rats: discrepancy between meta-analysis and a three-centre in vivo study" Cardiovascular Research, (2023) Jan 31:cvad024.

IF: 10.2

XVII. Onódi Z., Visnovitz T., Kiss B., Hambalkó S., Koncz A., Ágg B., Váradi B., Tóth V.E., Nagy R.N., **Gergely T.G.**, Gergő D., Makkos A., Pelyhe C., Varga N., Reé D., Apáti Á., Leszek P., Kovács T., Nagy N., Ferdinandy P., Buzás E.I., Görbe A., Giricz Z., Varga Z.V. "Systematic transcriptomic and phenotypic characterization of human and murine cardiac myocyte cell lines and primary cardiomyocytes reveals serious limitations and low resemblances to adult cardiac phenotype" J. Mol. Cell. Cardiol., (2022) vol. 165, pp. 19–30, Apr.

IF: 5.0

XVIII. Vörös I.; Onódi Z.; Tóth V.É.; **Gergely T.G.**; Sághy É.; Görbe A.; Kemény Á.; Leszek P.; Helyes Z.; Ferdinandy P.; Varga Z.V. "Saxagliptin Cardiotoxicity in Chronic Heart Failure: The Role of DPP4 in the Regulation of Neuropeptide Tone." Biomedicines (2022), 10, 1573.

IF: 4.7

XIX. Weber B.Y.; Brenner G.B.; Kiss B.; **Gergely T.G.**; Sayour N.V.; Tian H.; Makkos A.; Görbe A.; Ferdinandy P.; Giricz Z. "Rosiglitazone Does Not Show Major Hidden Cardiotoxicity in Models of Ischemia/Reperfusion but Abolishes Ischemic Preconditioning-Induced Antiarrhythmic Effects in Rats In Vivo." Pharmaceuticals (2022), 15, 1055.

IF: 4.6

XX. Brenner G. B., Giricz Z., Garamvölgyi R., Makkos A., Onódi Z., Sayour N. V., **Gergely T. G.**, Baranyai T., Petneházy Ö., Kőrösi D., Szabó G. P., Vago H., Dohy Z., Czimbalmos C., Merkely B., Boldin-Adamsky S., Feinstein E., Horváth I. G., Ferdinandy P. "Post-Myocardial Infarction Heart Failure in Closed-chest Coronary

Occlusion/Reperfusion Model in Göttingen Minipigs and Landrace Pigs." J. Vis. Exp. (2021) (170), e61901,

IF: 1.4

XXI. Brenner G., Makkos A., Nagy CT., Onódi Z., Sayour V.N., **Gergely T.G.**, Kiss B., Görbe A., Sághy É., Zádori Z., Lázár B., Baranyai T., Varga R., Husti Z., Varró A., Tóthfalusi L., Schulz R., Baczkó I., Giricz Z., Ferdinandy P. "Hidden cardiotoxicity of rofecoxib can be revealed in experimental models of ischemia/reperfusion" Cells, (2020) Feb 26;9(3):551.

IF: 6.6

∑IF: 135.0

10 ACKNOWLEDGEMENTS

The work was supported by the European Union's Horizon 2020 Research and Innovation Programme under grant agreement no. 739593 and by a Momentum Research Grant from the Hungarian Academy of Sciences (LP-2021-14 to ZVV). Project no. RRF-2.3.1-21-2022-00003 has been implemented with the support provided by the European Union. NVKP_16-1-2016-0017 ("National Heart Program") has been implemented with the support provided from the National Research, Development and Innovation Fund of Hungary. The research was financed by the Thematic Excellence Programme (2020-4.1.1.-TKP2020) of the Ministry for Innovation and Technology in Hungary, within the framework of the Therapeutic Development and Bioimaging thematic programmes of the Semmelweis University, by grants VEKOP-2.3.2-16-2016-00002 and VEKOP-2.3.3-15-2016-00006, and by 2020-1.1.6-JÖVŐ-2021-00013 ("Befektetés a jövőbe" NKFIH). This project was supported by grants from the National Research, Development, and Innovation Office (NKFIH) of Hungary (K134939 to TR, FK134751 to ZVV). I was supported by "Semmelweis 250+ Kiválósági PhD Ösztöndíj" (EFOP-3.6.3-VEKOP-16-2017-00009) and by Gedeon Richter Talentum Foundation's scholarship.

First of all, I am thankful to my supervisors and mentors during my PhD work, Dr. Zoltán Varga and Dr. Zoltán Giricz, who taught and guided me with inspiring mentorship throughout these years.

I am thankful to Prof. Péter Ferdinandy for the opportunity to work at an Institute which enables and requires the pursuit of the highest quality of research.

I also would like to thank Dr. Gábor Brenner, my supervisor during my undergraduate research work, whose mentorship has prepared me for my PhD years.

I am thankful for the immense support, patience, and work of Dr. Viktória Tóth.

I am thankful to my colleague and friend, Dr. Nabil Sayour, with whom I shared my scientific journey from the very first day.

I am grateful for all members of the Cardiovascular and Metabolic Group, HCEMM Cardiometabolic Immunology Research Group and MTA Momentum Cardio-oncology and

Cardio-immunology Research Group of Semmelweis University, as it would not have been possible to perform these studies without teamwork, including Dr. Dániel Kucsera, Dr. Zsófia Gulyás-Onódi, Dr. Imre Vörös, Tamás Kovács, Dr. Bence Ágg, Dr. Balázs Petrovich, Dr. Csenger Kovácsházi and Regina Nagy, among others.

I am grateful to our collaborators at the Városmajor Heart and Vascular Center, Dr. Zsófia Drobni, Dr. Mihály Ruppert, Dr. Tamás Radovits and Prof. Béla Merkely.

I am also thankful to Dr. András Makkos and Dr. Anikó Görbe for the mentorship at various stages of my undergraduate and PhD research work.

Finally, I am very thankful to my family, especially to my Mom, for the unconditional support I have received that enabled me to pursuit my academic journey.